Dickinson and Company (BD), NJ, USA). Lymphocytes prepared from spleens were stimulated with TYRP-2 peptide (2 mg/ml) for five days, then stained with APC-labeled TYRP-2-specific tetramer and FITC-labeled CD8a mAb. Samples were analyzed by FACS vantage using Cell QUEST software (BD). Lymphocytes were gated on $CD8^+$ cells. More than 10^5 events were acquired for each sample.

2.8. Cell proliferation assay

For assessment of the growth-inhibitory activities of NPr-4-*S*-CAP and NPr-2-*S*-CAP, NIH3T3, B16F1, 70W and M1 cells were dispensed at a density of 1.0×10^5 in 6-cm dishes and cultured for 24 h. Selected concentrations of NPr-4-*S*-CAP (0.5, 1.0, 2.0, and 3.0 mM), NPr-2-*S*-CAP (0.5, 1.0, 2.0, and 3.0 mM) or propylene glycol (120 μl) were added. After cells were cultured for 1 h, they were washed and refed with fresh DMEM and cultured for 24 h. The numbers of living cells that were not stained by trypan blue were counted and the average of 6 dishes was determined.

2.9. Flow cytometric analysis

B16F1, NIH3T3, RMA and TXM18 cells were cultured in the NPr-4-*S*-CAP-containing medium (1 mM) or propylene glycol for 1 h, they were washed in PBS and cultured for 24 h. For the positive control of apoptosis, TNF-related apoptosis-inducing ligand (TRAIL)/Apo2L (Wako, 2.0 μg/ml) was added and the cells were cultured for 24 h. Next, adherent and floating cells were collected together, washed in PBS, dehydrated in 70% cold ethanol and stored on ice for 2 h. They were then rehydrated in cold PBS and incubated in the presence of RNaseA (100 μg/ml) (Invitrogen) at 37 °C for 30 min. After incubation, the cells were rinsed twice in cold PBS and suspended in 2.0 ml of PBS containing 10 μg/ml propidium iodide (Wako) at 4 °C for 2 h. Sub G1, G1, S, and G2/M populations were quantified with a FACS Calibur flow cytometer (BD) using the Cell QUEST program.

2.10. Caspase enzyme assay

For this assay, 1.5×10^4 B16F1, NIH3T3, RMA and TXM18 cells were seeded in 96-well plates. After 24 h, the medium was replaced by one containing NPr-4-*S*-CAP or propylene glycol at the indicated concentrations followed by incubation for 1 h at 37 °C and washing with PBS. For positive control, cells were cultured in the presence of TRAIL/Apo2L and cultured for 24 h. After medium containing Caspase-Glo3/7 Assay kit solution (100 μl, Promega, Madison, WI) was added and the cells were cultured for 2 h, activity of caspase 3/7 was measured using a Wallac 1420 ARVO series multilabel reader (Perkin Elmer, MA, USA).

2.11. TUNEL assay

In order to assess the apoptosis in NPr-4-*S*-CAP mediated melanoma tumors, TUNEL assay was performed with an apoptosis detection kit (Takara Bio, Shiga, Japan). Tumors in group III and control groups processed according to Protocols 1 and 3 were harvested on day 22 as described above and fixed in formalin (4%, w/v) overnight. Samples were then dehydrated and embedded with paraffin. The staining was operated according to the manufacturer's instructions.

2.12. Fluorescence microscopy

Using a confocal fluorescence microscope (Radiance 2000MP, BIO-RAD, CA, USA), we studied the morphologic features of cell death induced by NPr-4-*S*-CAP. For this, 1.5×10^4 B16F1 and NIH3T3 cells were separately seeded on round glass coverslips that were coated with Atelo Cell IPC-30 (Koken Co. Ltd., Tokyo, Japan) and put into 12-well plates. They were cultured for 24 h with 5% FBS at 37 °C in a 5% CO_2 atmosphere. Cells were stained with 5 μM 5-(and-6)-chloromethyl-2′,7′-dichlorodihydro-fluorescein diacetate, acetyl ester (CM-H_2DCFDA, Invitrogen) for 30 min. They were then cultured in the medium containing NPr-4-*S*-CAP (1.0 mM) or propylene glycol (40 μl) for 1 h. After being cultured for 24 h, they were stained with a Rab pAb to Active Caspase 3 (Abcam, Cambridge, MA, USA), stained with Hoechst 33342 (10 μl per dish, Wako, Japan) and analyzed under a confocal microscope. The difference between apoptosis and necrosis was determined according to a previous report [15]; cells with nuclei showing aggregation and deformation were considered to be apoptotic and those with round nuclei to be necrotic.

2.13. Detection and analysis of intracellular ROS

After non-pigmented melanoma TXM18 and SK-mel-24 cell lines and pigmented melanoma B16F1, 70W, M-1 and G361 cells were cultured in medium containing 5 μM CM-H_2DCFDA (DCF, Invitrogen) for 30 min at 37 °C, they were washed with PBS, refed with medium containing NPr-2-*S*-CAP (1, 3, 6 mM) or NPr-4-*S*-CAP (0.5, 1, 2, 3, or 6 mM). After they were cultured for 1 h, they were washed in PBS and cultured for 24 h. For the positive control with exposure to ROS, the cells were cultured with H_2O_2 (0.5, 1, 2, 3 mM) for 24 h. Next, adherent and floating cells were collected together and processed for flow cytometry to quantify the M2 fraction using the Cell QUEST program (BD).

2.14. Statistical analyses

The data were analyzed by one- or two-way analysis of variance (ANOVA) and then differences in experimental results for tumor growth were assessed by Sheffe's test to compare all the experimental groups, or Dunnett's test for the experimental groups vs. the control group. For multiple comparisons the data were assessed by the log-rank test with Bonferroni correction. Differences in survival rates were analyzed by the Kaplan–Meier method. The level of significance was $P < 0.05$ (two-tailed). All statistical analyses were performed using StatView J-5.0 (SAS Institute Inc., Cary, NC, USA).

3. Results

3.1. NPr-4-S-CAP induces apoptotic cell death of B16F1 cells

B16F1, 70W and M-1 melanoma and NIH3T3 fibroblast cells were separately cultured in media containing different concentrations of NPr-4-*S*-CAP (0–3.0 mM) and NPr-2-*S*-CAP (0–3.0 mM). After a 24 h-incubation period, the anti-proliferative effect was assessed by cell-counting assay. Fig. 1 shows the effects of different concentrations of NPr-4-*S*-CAP and NPr-2-*S*-CAP on melanoma and NIH3T3 cells. The results indicated that NPr-4-*S*-CAP had a dose-dependent antiproliferative effect on B16F1, 70W and M-1 cells ($P < 0.05$, 51.6% of the relative cell number at the concentration of 3.0 mM in B16F1 cells) but not on NIH3T3 cells (83.7% at 3.0 mM). Conversely, NPr-2-*S*-CAP, an inactive form of CAP, did not have antiproliferative effects on B16F1 or NIH3T3.

To examine the mechanism of the cell death induced by NPr-4-*S*-CAP, these cells were subjected to flow cytometric analysis, caspase 3 assay and TUNEL staining. The sub-G1 fraction was increased in the NPr-4-*S*-CAP-treated B16F1 cells, comparable to TRAIL-exposed B16F1, but not in the NPr-4-*S*-CAP-treated non-melanoma cells (NIH3T3, RMA) or non-pigmented melanoma cells (TXM18) (Fig. 2A). The luminescent assay detected caspase 3/7 activity in the NPr-4-*S*-CAP-treated B16F1 cells remarkably

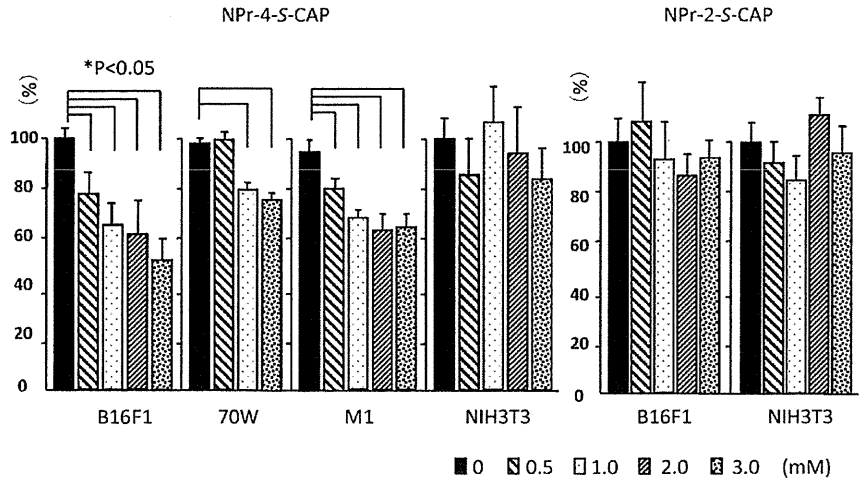

Fig. 1. NPr-4-*S*-CAP, but not NPr-2-*S*-CAP, suppresses growth of melanoma cells. The number of cells cultured in the medium containing NPr-4-*S*-CAP or NPr-2-*S*-CAP was counted as described in Section 2. All data are presented as mean ± standard deviation. Growth of B16F1, 70W and M-1 melanoma, but not NIH3T3 fibroblast cells, was suppressed by NPr-4-*S*-CAP ($P < .05$, Dunnett's test).

increased (35.8-fold) compared to that in the non-treated cells (Fig. 2B). NIH3T3, RMA and TXM18 cells treated with TRAIL showed 10.6, 7.1 and 5.8-fold increases of caspase 3/7 activation compared to the control, respectively, whereas those with NPr-4-*S*-CAP showed increases of 4.1, 1.4 and 1.8-fold, respectively (Fig. 2B). As shown in Fig. 2C, the number of TUNEL-positive cells was significantly increased only in the B16F1 tumor treated with NPr-4-*S*-CAP. This increase was not observed in the B16F1 tumor without NPr-4-*S*-CAP or in RMA tumors with or without NPr-4-*S*-CAP. These findings suggested that NPr-4-*S*-CAP induces apoptotic cell death selectively in pigmented melanoma cells.

3.2. NPr-4-S-CAP produces ROS

Melanoma cells produce ROS in the process of melanogenesis, possibly resulting in their degradation with disruption of cell

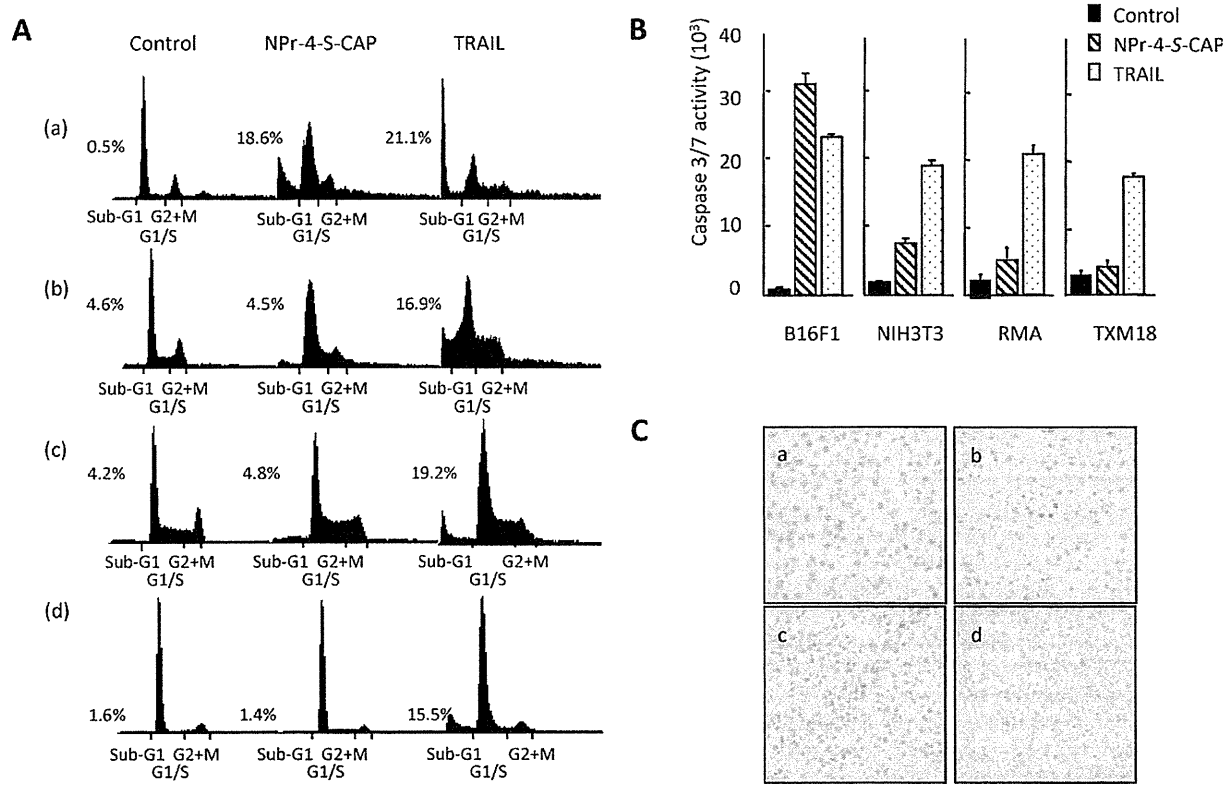

Fig. 2. NPr-4-*S*-CAP mediated apoptotic cell death of B16F1 melanoma cells. (A) Flow cytometric analysis of cellular DNA detected an increased sub-G1 fraction in NPr-4-*S*-CAP-treated B16F1 (a), but not NIH3T3 (b), RMA (c) or TXM18 (d). (B) Assay of caspase 3/7 in cells treated with NPr-4-S-CAP or TRAIL. Cells were cultured in the presence of NPr-4-S-CAP, TRAIL, or propylene glycol in 96-well plates and then processed for measurement of caspases 3 and 7 using a Caspase-Glo3/7 Assay kit. (C) Apoptosis of B16F1 tumors induced by NPr-4-*S*-CAP was assessed by the TUNEL method. Samples were obtained from (a) B16F1 tumors injected with propylene glycol, (b) B16F1 tumors treated with NPr-4-*S*-CAP, (c) RMA tumors injected with propylene glycol and (d) RMA injecteds with NPr-4-*S*-CAP. TUNEL-positive nuclei appear dark brown (200×).

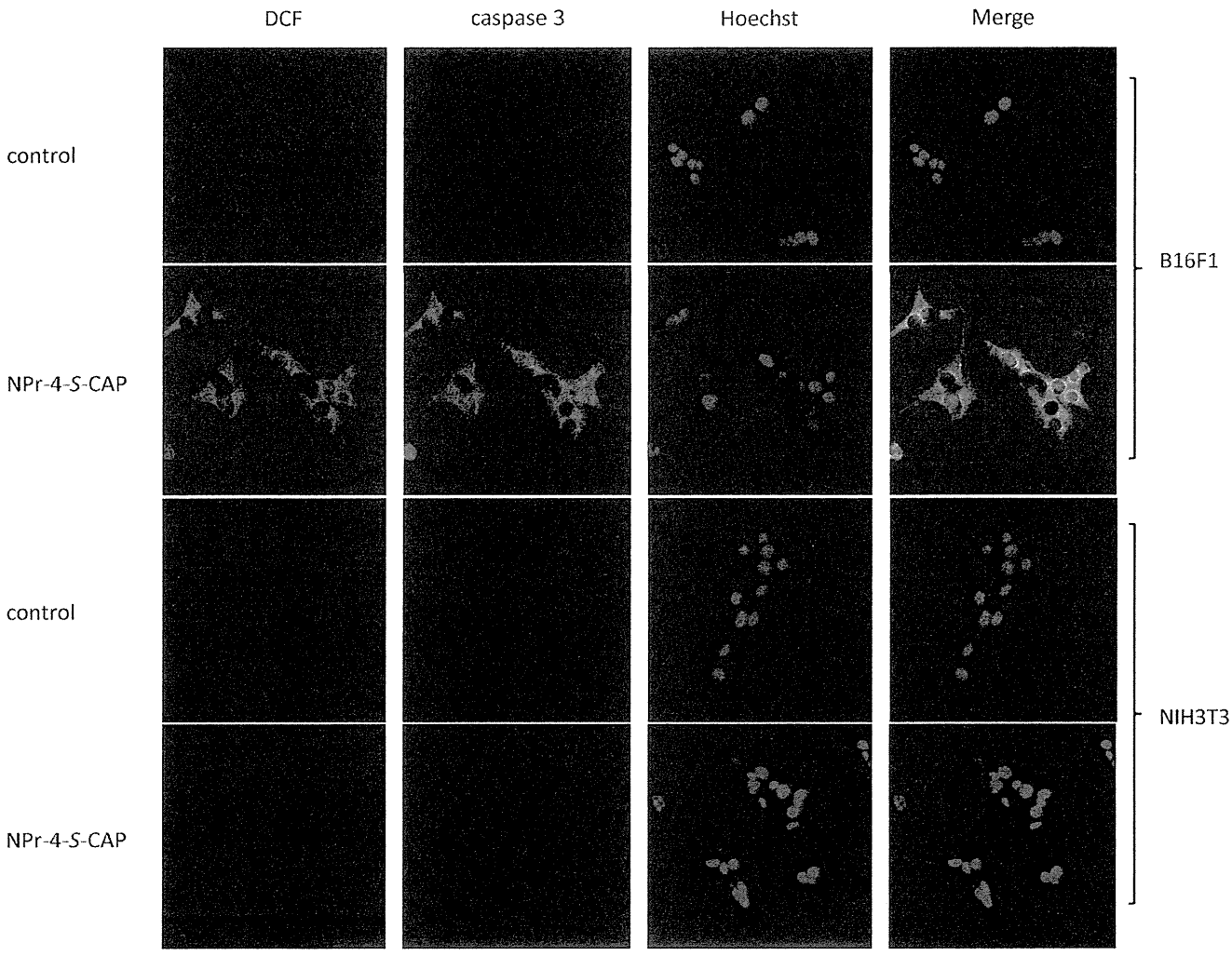

Fig. 3. Confocal microscopic observation of cells treated with NPr-4-*S*-CAP. B16F1 and NIH3T3 cells were stained with CM-H_2DCFDA for ROS production, a Rab pAb for activated caspase 3, and Hoechst 33342 for living nuclei.

membranes [16–18], but the molecular mechanism of NPr-4-*S*-CAP-mediated cell death has not yet been elucidated. To analyze the relations between NPr-4-*S*-CAP-mediated apoptosis and ROS production in B16F1 cells, we examined ROS generation and morphological changes using confocal fluorescent microscopy and flow cytometer. When B16F1 cells were cultured in the medium containing NPr-4-*S*-CAP, about half of their nuclei were aggregated and deformed, which was associated with an increase of ROS and caspase 3 in their cytoplasm (Fig. 3). NIH3T3 cells, however, did not show any of these changes (Fig. 3). When pigmented (B16F1, 70W, M-1 and G361) and non-pigmented (TXM18 and SK-mel-24) melanoma cells were treated with NPr-4-*S*-CAP, ROS production was selectively observed in the pigmented melanoma cell lines (Fig. 4). These findings suggested that NPr-4-*S*-CAP selectively produced ROS in pigmented melanoma cells such as B16F1 and that ROS played an important role in the NPr-4-*S*-CAP-associated apoptosis.

3.3. NPr-4-S-CAP suppresses growth of primary and secondary B16F1 tumors in mice

To examine whether NPr-4-*S*-CAP had an anti-melanoma effect, syngeneic mice bearing B16F1 tumors were given NPr-4-*S*-CAP by intratumoral injections and the volumes of tumors are measured as described in Section 2. First, we compared the direct effects of NPr-4-*S*-CAP and NPr-2-*S*-CAP on the transplanted B16F1 melanomas. Growth of tumors injected with NPr-4-*S*-CAP was remarkably suppressed ($P = .0247$ by a Sheffe test), but those treated with NPr-2-*S*-CAP, like control mice, were not affected (Fig. 5). The mice were divided into four different groups, a non-treated control group, and treated groups I, II and III. Tumors in group II (injected every other day for a total of five times) and group III (injected for five consecutive days), especially, showed significant reductions in their volumes compared to those of control mice by day 20 ($P = .0163$ and .0100, respectively, vs. control group, Fig. 6A). On the other hand, NPr-4-*S*-CAP did not affect the tumor volume of transplanted RMA T-cell lymphoma (Fig. 6B). These results suggested that NPr-4-*S*-CAP had a selective chemotherapeutic effect on B16F1 melanoma cells.

We then examined whether secondary B16F1 tumors transplanted on the opposite flank were suppressed after the treatment of primary tumors with NPr-4-*S*-CAP. In all the treated groups (I, II and III), tumor growth after being re-challenged with secondary B16F1 melanomas was suppressed (Fig. 6C). The tumor volumes of groups II and III were significantly reduced compared to those of the control mice ($P = .0321$ and .0160, respectively, Fig. 6C).

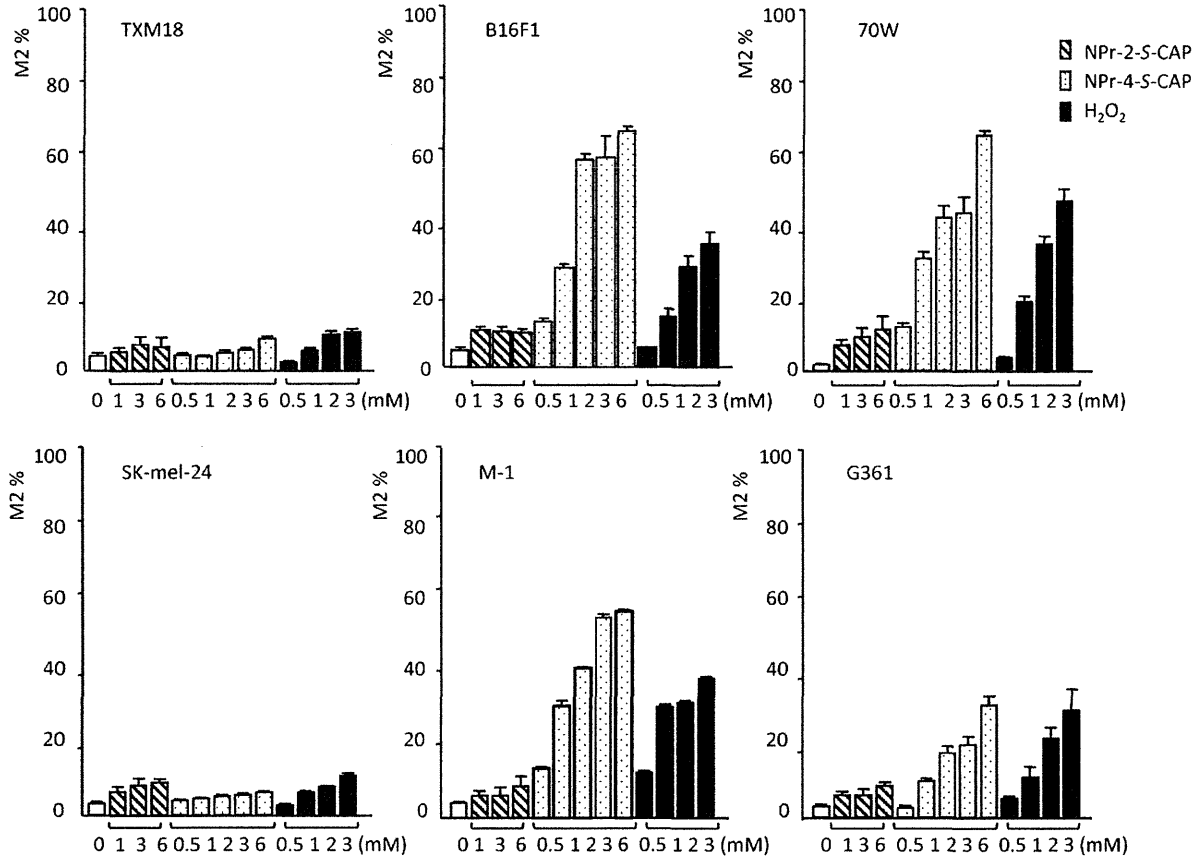

Fig. 4. Pigmented melanoma but not non-pigmented melanoma cells produce ROS in the presence of NPr-4-*S*-CAP. Cells were cultured in the presence of MDCF for 30 min, washed twice with PBS, refed with medium containing NPr-2-*S*-CAP or NPr-4-*S*-CAP and cultured for a further 1 h. They were then harvested and processed for FACScan analysis.

However, secondary RMA T-cell lymphoma tumors were not suppressed when they were transplanted after the primary B16F1 tumors were removed (Fig. 6D). The survival periods and survival rates of mice among the four groups were observed for as long as 120 days. Significant prolongations of survival were observed in groups I, II and III compared to the control group ($P = .0177, .0024$ and .0435, respectively, Fig. 7A).

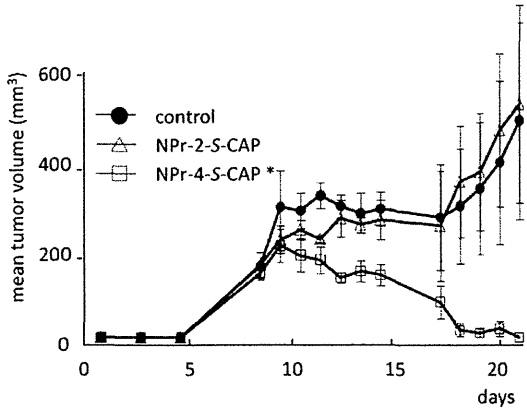

Fig. 5. NPr-4-*S*-CAP, but not NPr-2-*S*-CAP, suppresses growth of transplanted B16F1 tumors. The syngeneic mice bearing B16F1 tumors were given 24.4 μmol NPr-4-*S*-CAP or NPr-2-*S*-CAP in five consecutive intratumoral injections and the volumes of tumors were measured.

In the histopathological examination against primary and secondary transplanted B16F1 or RMA tumors, a dense inflammatory infiltrate including neutrophils, macrophages, plasma cells and lymphocytes was observed around NPr-4-*S*-CAP treated B16F1 tumors which were harvested on day 22 (Fig. 8E and F). Furthermore, we observed that numerous $CD8^+$ T cells were infiltrated within these tumors (Fig. 8H). By contrast, inflammatory cells were not detectable in the primary B16F1 tumors without treatment or RMA tumors with or without treatment (Fig. 8A and B, data not shown for RMA tumors). $CD4^+$ T cells were not infiltrated in either these tumors (Fig. 8C and G). In the secondary B16F1 tumors, the inflammatory cells were infiltrated around the residual tumor but the density of $CD4^+$ and $CD8^+$ T cells was not prominent as the treated primary tumors (data not shown).

3.4. $CD8^+$ T cells mediate suppression of re-challenged B16F1 melanoma

Six weeks after the NPr-4-*S*-CAP injections, vitiligo (depigmented cutaneous lesions) or a change in hair color to white appeared in two of the six mice in group III in the areas of the body distant from the injection points (Fig. 7B). This suggested that the vitiligo was not generated by a direct effect of NPr-4-*S*-CAP but by the induction of systemic tumor-specific T-cell immunity against melanocytes. To analyze the mechanism of the anti-melanocyte immunity induced by NPr-4-*S*-CAP, in vivo T cell depletion assay was performed. When B16F1 melanoma-bearing mice were injected with an anti-CD8 antibody i.p., tumor growth was not

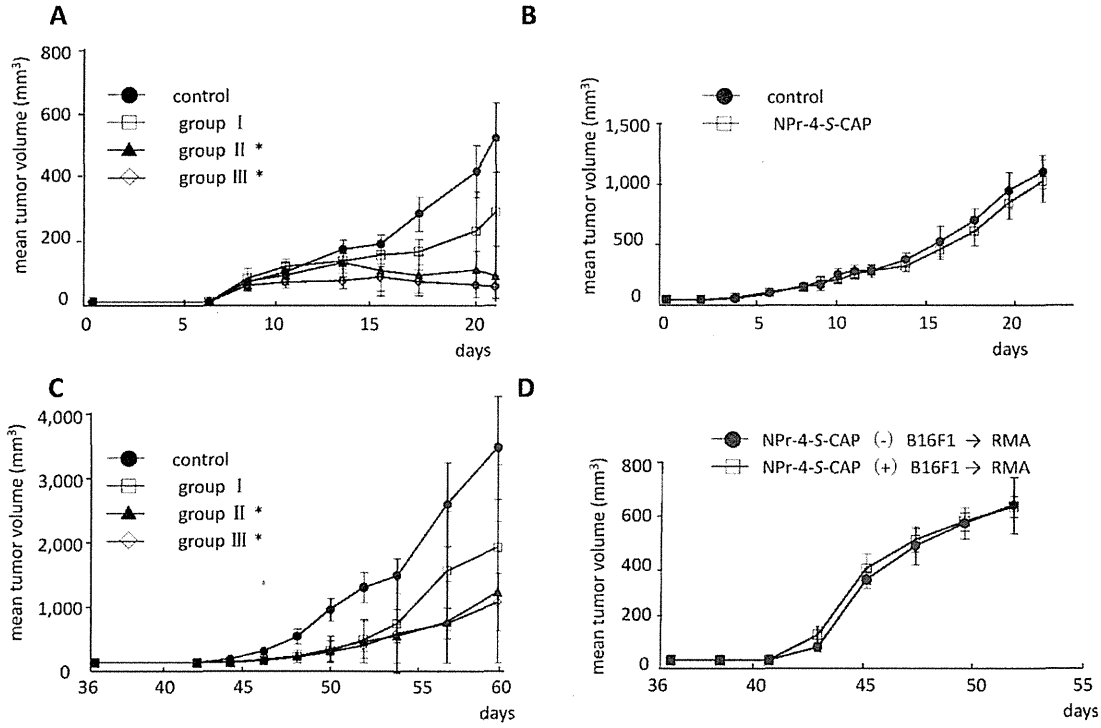

Fig. 6. NPr-4-*S*-CAP suppresses growth of primary and secondary rechallenge B16F1 melanomas. (A) Mice were transplanted with B16F1 cells and treated with NPr-4-*S*-CAP. Tumor volumes of treated groups I, II and III were suppressed. In particular, tumors in groups II and III showed significant reductions in their volumes ($P < .05$). (B) Transplanted RMA mouse T lymphomas were injected with NPr-4-*S*-CAP and tumor volumes were measured. (C) Tumor volumes of secondary B16F1 melanomas in mice belonging to groups I, II and III. Growth of rechallenge melanomas on the opposite flanks was markedly suppressed in the mice of groups II and III. (D) Growth of secondarily transplanted RMA lymphomas was not inhibited in mice after the primary B16F1 tumors were removed.

suppressed. However, the growth of tumors remained significantly suppressed (i.e., it was not further affected) after injection of an anti-CD4 antibody or Rat IgG i.p. ($P = .0167$ vs. rat IgG group, Fig. 9). This suggested that $CD8^+$ T cells participated in the NPr-4-*S*-CAP-mediated anti-B16F1 immunity.

To analyze whether tumor-specific immunity had been induced, CTL induction was examined by Cr-release assay and tetramer assay. Spleen cells were obtained from the cured mouse and mixed with B16F1 cells to detect their specific lyses. As shown in Fig. 10A, spleen cells showed cytotoxic activity to B16F1 cells but not to the non-melanoma RMA cells. However, spleen cells from the naïve or RMA-challenged mice did not show cytotoxic activity to either B16F1 or RMA cells. For the tetramer assay, splenocytes were prepared from a naïve mouse and from mice with B16F1 or RMA tumors after treatment with NPr-4-*S*-CAP, and stimulated in vitro with TYRP-2 peptide for five days.

Recovered splenocytes were stained with TYRP-2-specific tetramer, and proportions of peptide-specific $CD8^+$ T cells were

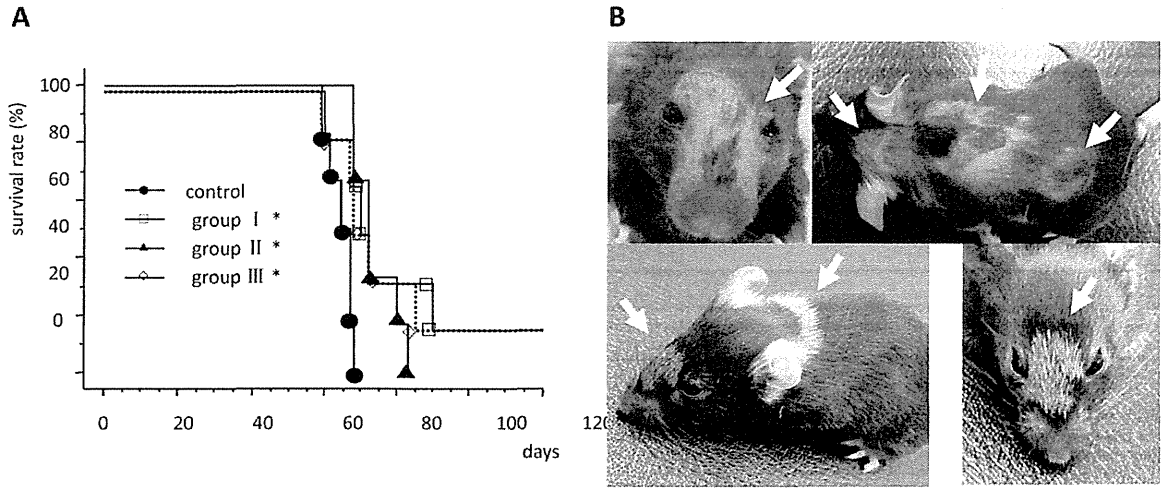

Fig. 7. (A) The survival periods and survival rates of tumor-bearing mice. Kaplan–Meier survival curves over a period of 120 days after the tumor transplantation showed that significant prolongations of survival were observed in groups I, II and III compared to the control mice ($P = .0177$, $P = .0024$ and $P = .0435$, respectively, vs. control). (B) Appearance of vitiligo on the treated mice. Six weeks after the NPr-4-*S*-CAP injection, vitiligo or white hair appeared at body sites distant from the injection point.

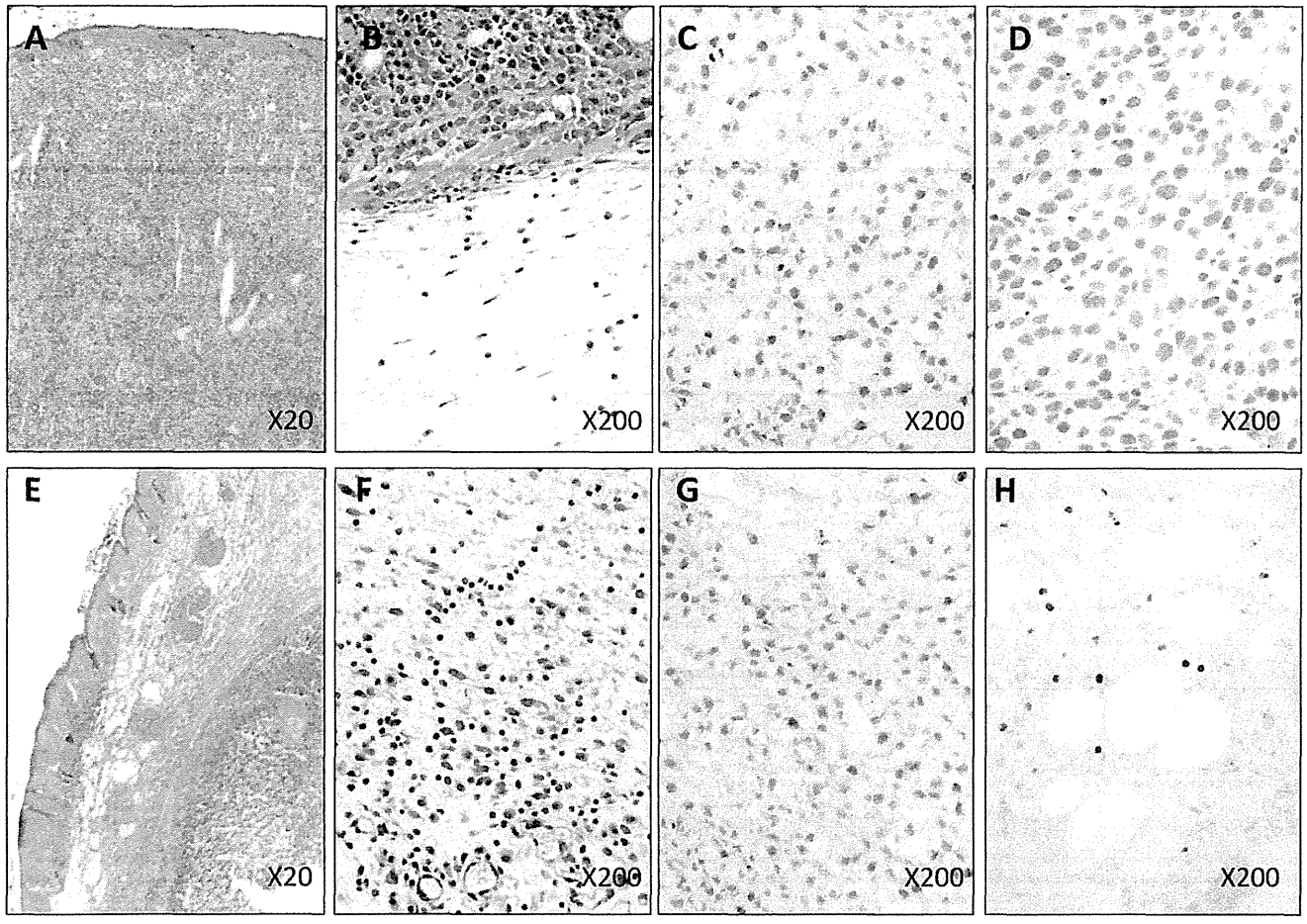

Fig. 8. Dense inflammatory cells and CD8$^+$ T cells were infiltrated in NPr-4-*S*-CAP treated B16F1 tumors. The B16F1 tumors were harvested on day 22 and histopathological features were analyzed by HE-staining (A, B, E, F) or an anti-mouse CD4 mAb (C, G) or CD8 mAb (D, H).

determined. As shown in Fig. 10B, 9.08% of the CD8$^+$ T cells in the B16F1-challenged mice treated with NPr-4-*S*-CAP were specific for the TYRP-2 peptide, compared with 2.66% or 2.96% in the naïve or RMA-challenged mice, respectively. In addition, lymphocytes isolated from the regional lymph node of RMA or B16F1 transplanted into mice treated with NPr-4-*S*-CAP, were also stained with TYRP-2-specific tetramer. As shown in Fig. 10B, 8.14% of the CD8$^+$ T cells in the B16F1-challenged mice treated with NPr-4-*S*-CAP were specific for the TYRP-2 peptide, compared with 5.43% or 4.89% in the naïve or RMA-challenged mice, respectively.

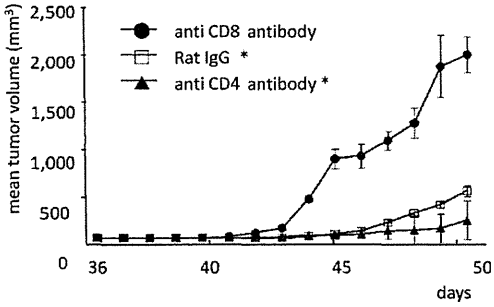

Fig. 9. Suppression of secondary tumors is inhibited by an anti-CD8 antibody. After the first challenge, the mice from group III were injected with 0.2 mg of anti-CD4, anti-CD8 or rat IgG i.p. on days 29 and 43, one week before and after the rechallenge by B16F1 transplantation, respectively.

The results from the two independent CTL assays were highly consistent, showing that the NPr-4-*S*-CAP treatment to B16F1 melanoma produced a functional CTL response.

4. Discussion

Although selective cytotoxicities and anti-melanoma effects of cysteaminyl phenol derivatives have been reported, the mechanisms of cell death induced by the compounds have not been elucidated. Here, we demonstrated that NPr-4-*S*-CAP induced apoptosis selectively in pigmented melanoma cells in association with ROS production and caspase 3 activation. In addition, this is the first report demonstrating that NPr-4-*S*-CAP can induce host T-cell immune responses associated with rejection of in vivo rechallenge with melanoma.

Tyrosinase inhibitors with simple skeletal structures similar to phenol such as hydroquinone, kojic acid, arbutin and deoxyarbutin have been used as skin whitening agents via topical application [19]. Administration of a melanin precursor such as 4-*S*-cysteaminylphenol to black mice resulted in depigmentation of hair follicles, possibly by the selective disintegration of melanocytes in the hair bulb [10,14,20–22]. NPr-4-*S*-CAP exerts strong cytotoxicity toward melanoma cells, in which melanin synthesis is highly elevated [8,9,11]. When phenolic amine compounds are oxidized by tyrosinase, melanin intermediates inhibit the activity of SH enzymes such as thymidylate synthase, alcohol dehydrogenase and DNA polymerase by covalent binding through their

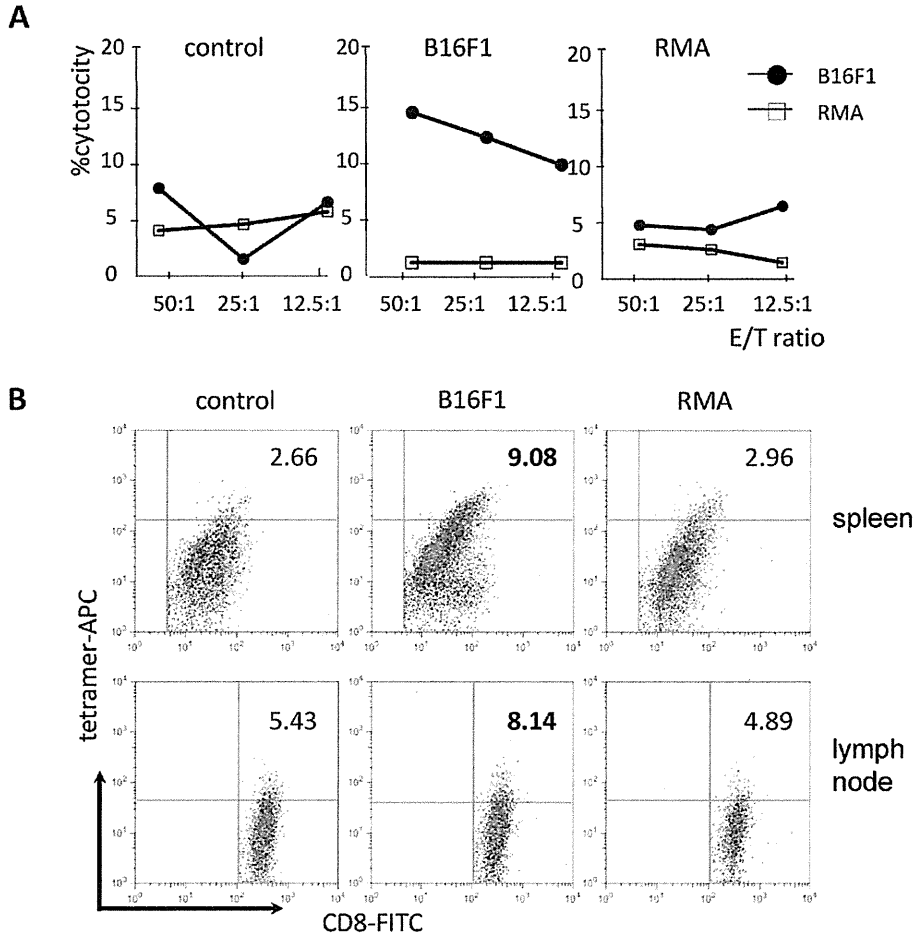

Fig. 10. Splenocytes and/or lymphocytes of tumor-bearing mice contain CTL activity against B16F1 cells detectable by ^{51}Cr assay (A) and tetramer assay (B). (A) After the first challenge, the spleen cells from naïve mice (control) and B16F1- or RMA-challenged mice treated with NPr-4-*S*-CAP were harvested from the mice and cytotoxic activity of effector cells against target cells (B16F1 and RMA) was determined by standard ^{51}Cr assay. T, tumor B16F1 cells; E, effector spleen cells. (B) Splenocytes and lymphocytes from naïve mice (control), RMA- or B16F1-challenged mice treated with NPr-4-*S*-CAP were stained with APC-labeled TRP-2-specific tetramer together with FITC-labeled anti-CD8 mAb. The numbers shown represent the percentage of tetramer$^+$ cells within CD8$^+$ T lymphocytes.

cysteine residues, resulting in melanoma-specific cytotoxicity [23–25].

In the present study, NPr-4-*S*-CAP suppressed growth of cultured melanoma cells and induced apoptotic cell death accompanied by ROS generation. Since pigmented melanoma cells (B16F1, 70W, G361 and M-1), but not non-pigmented ones (TXM18 and SK-mel-24), produced significant amounts of ROS (Fig. 4) in the presence of NPr-4-*S*-CAP, it was suggested that melanin biosynthesis was essential for NPr-4-*S*-CAP to produce ROS. It has been reported that ROS-mediated apoptosis is initiated via two pathways, the death receptor (Fas ligand–Fas receptor) and the mitochondria-mediated pathway in which the Trx/ASK1 complex acts as a redox switch to release cytochrome C [26,27]. Intracellular ROS mediate apoptotic cell death, which elicits a strong host inflammation reaction and subsequent induction of host immune responses [28]. Transcription factor NF-E2-related factor 2 (Nrf2) is activated by ROS to induce cellular genes such as glutathione-*S*-transferase, heme oxygenase and glucose-6-phosphodehydrogenase to protect cells from oxidative stress [29,30]. It is possible that Nrf2-1 and/or its related genes could not be induced to a level sufficient for the protection of melanoma cells from oxidative stress.

In the mouse model of thermotherapy for B16 melanoma, it has been suggested that HSPs, especially HSP70 and HSP72, are involved in tumor-specific CTL responses [31,32]. We suggested in a previous report that the CTL response against B16-OVA melanoma induced by hyperthermia using NPrCAP/M (NPr-4-*S*-CAP conjugated to magnetite) was associated with the release of the HSP72-peptide complex from degraded tumor cells [33]. In the present study, we therefore examined whether HSPs were induced in and released from melanoma cells after injection of NPr-4-*S*-CAP; however, Western blot analysis did not detect an increase of HSP72 or HSP90 in the NPr-4-*S*-CAP-treated B16F1 cells (data not shown). Thus, although intracellular HSPs may play a role in the induction of NPr-4-*S*-CAP-mediated antitumor immunity, the induction of HSPs is not a prerequisite for the NPr-4-*S*-CAP-mediated tumor-specific immune response.

Results of the in vivo T cell depletion assay using anti-CD8 antibodies, Cr-releasing assay and tetramer assay using B16F1 and spleen cells from NPr-4-*S*-CAP-treated and cured mice suggested that suppression of the primary tumor by NPr-4-*S*-CAP was able to induce CD8$^+$ T cell immunity against component of B16F1 melanoma. Melanoma tumor antigens recognized by T lymphocytes are derived from melanocyte differentiation antigens (tyrosinase, TYRP-1, TYRP-2 and gp100), tumor testis antigens (NY-ESO-1, MAGE1 and MEGE3) and mutated cellular gene products (β-catenin and p53). In mouse B16 melanoma model, TYRP-2 is reported to be a strong melanoma rejection antigen since

tolerance to TYRP-2 can be broken by TYRP-2 vaccination and TYRP-2-specific CTCLs mediate anti-tumor immunity [34–36]. Although it is not clear which B16F1 tumor antigens were presented on the dendritic cells for induction of $CD8^+$ T cells, in comparison with the naïve or RMA-transplanted mice, increased frequency of $CD8^+$ T cells specific for the TYRP-2 peptide were detected in B16F1-challenged mice treated with NPr-4-S-CAP. This suggested that TYRP-2 was a part, but not all, of a tumor antigen associated with rejection of B16 melanoma.

Recently, Westerhof et al. proposed the haptenation theory in which increased intracellular H_2O_2 could trigger the increased turnover of elevated levels of surrogate substrates of tyrosinase, resulting in melanocyte-specific T-cell responses [37,38]. According to this hypothesis, tyrosinase would be recognized as a melanoma-specific tumor antigen in relation to the systemic immune responses. This line of study may contribute to the clinical application of NPr-4-S-CAP for therapy targeting malignant melanoma.

Acknowledgments

This work was supported by Health and Labor Sciences Research Grants-in-Aid (H17-nano-004 and H21-nano-006) for Research on Advanced Medical Technology from the Ministry of Health, Labor and Welfare of Japan.

References

[1] Ishihara K, Saida T, Otsuka F, Yamazaki N. Prognosis and Statistical Investigation Committee of the Japanese Skin Cancer Society. Statistical profiles of malignant melanoma and other skin cancers in Japan: 2007 update. Int J Clin Oncol 2008;13:33–41.
[2] Balch CM, Gershenwald JE, Soong SJ, Thompson JF, Atkins MB, Byrd DR, et al. Final version of 2009 AJCC melanoma staging and classification. J Clin Oncol 2009;27:6199–206.
[3] Rad HH, Yamashita T, Jin HY, Hirosaki K, Wakamatsu K, Ito S, et al. Tyrosinase-related proteins suppress tyrosinase-mediated cell death of melanocytes and melanoma cells. Exp Cell Res 2004;298:317–28.
[4] Jimbow K, Miura S, Ito Y, Kasuga T, Ito S. Utilization of melanin precursors for experimental chemotherapy of malignant melanoma. Jpn J Cancer Chemother 1984;11:2125–32.
[5] Ito S, Kato T, Ishikawa K, Kasuga T, Jimbow K. Mechanism of selective toxicity of 4-S-cysteinylphenol and 4-S-cysteaminylphenol to melanocytes. Biochem Pharmacol 1987;36:2007–11.
[6] Pankovich JM, Jimbow K, Ito S. 4-S-cysteaminylphenol and its analogues as substrates or tyrosinase and monoamine oxide. Pigment Cell Res 1990;3:146–9.
[7] Miura T, Jimbow K, Ito S. The in vivo antimelanoma effect of 4-S-cysteaminylphenol and its N-acetyl derivative. Int J Cancer 1990;46:931–4.
[8] Alena F, Iwashita T, Gili A, Jimbow K. Selective in vivo accumulation of N-acetyl-4-cysteaminylphenol in B16F10 murine melanoma effect by combination of buthionine sulfoximine. Cancer Res 1994;54:2661–6.
[9] Tandon M, Thomas PD, Shokravi M, Singh S, Samra S, Chang D, et al. Synthesis and antitumor effect of the melanogenesis-based antimelanoma agent N-propionyl-4-S-cysteaminylphenol. Biochem Pharmacol 1998;55:2023–9.
[10] Minamitsuji Y, Toyofuku K, Sugiyama S, Yamada K, Jimbow K. Sulfur containing tyrosine analogs can cause selective melanocytotoxicity involving tyrosinase-mediated apoptosis. J Invest Dermatol Symp Proc 1999;4:130–6.
[11] Thomas PD, Kishi H, Cao H, Ota M, Yamashita T, Singh S, et al. Selective incorporation and specific cytocidal effect as the cellular basis for the antimelanoma action of sulphur containing tyrosine analogs. J Invest Dermatol 1999;113:928–34.
[12] Sato M, Yamashita T, Okura M, Osai Y, Sato A, Takada T, et al. N-propionyl-cysteaminylphenol–magnetite conjugate (NPrCAP/M) is a nanoparticle for the targeted growth suppression of melanoma cells. J Invest Dermatol 2009; 129:2233–41.
[13] Eikawa S, Ohue Y, Kitaoka K, Aji T, Uenaka A, Oka M, et al. Enrichment of Foxp3+ CD4 regulatory T cells in migrated T cells to IL-6- and IL-8-expressing tumors through predominant induction of CXCR1 by IL-6. J Immunol 2010;185:6734–40.
[14] Miura S, Ueda T, Jimbow K, Ito S, Fujita K. Synthesis of cysteinylphenol, cysteaminylphenol, and related compounds, and in vivo evaluation of anti-melanoma effect. Arch Dermatol Res 1987;279:219–25.
[15] Shimizu S, Eguchi Y, Kamiike W, Itoh Y, Hasegawa J, Yamabe K, et al. Induction of apoptosis as well as necrosis by hypoxia and predominant prevention of apoptosis by Bcl-2 and Bcl-X_L. Cancer Res 1996;56:2161–6.
[16] Rotman A, Daly JW, Creveling CR. Oxygen-dependent reaction of 6-hydroxydopamine,5,6-dihydroxytryptamine and related compounds with proteins in vivo: a model for cytotoxicity. Mol Pharmacol 1976;12:887–99.
[17] Ito S, Inoue S, Fujita K. The mechanism of toxicity of 5-S-cysteinyldopa to tumour cells. Hydrogen peroxide as a mediator of cytotoxicity. Biochem Pharmacol 1983;32:2079–81.
[18] Yamada K, Jimbow K, Engelhardt R, Ito S. Selective cytotoxicity of a phenolic melanin precursor, 4-S-cysteaminylphenol, on in vitro melanoma cells. Biochem Pharmacol 1989;38:2217–21.
[19] Solano F, Briganti S, Picardo M, Ghanem G. Hypopigmenting agents: an updated review on biological, chemical and clinical aspects. Pigment Cell Res 2006;19:550–71.
[20] Ito Y, Jimbow K, Ito S. Depigmentation of black guinea pig skin by topical application of cysteaminylphenol, cysteinylphenol, and related compounds. J Invest Dermatol 1987;88:77–82.
[21] Ito Y, Jimbow K. Selective cytotoxicity of 4-S-cysteaminylphenol on follicular melanocytes of the black mouse: rational basis for its application to melanoma chemotherapy. Cancer Res 1987;47:3278–86.
[22] Jimbow K, Iwashina T, Alena F, Yamada K, Pankovich J, Umemura T. Exploitation of pigment biosynthesis pathway as a selective chemotherapeutic approach for malignant melanoma. J Invest Dermatol 1993;100:S231–8.
[23] Wick MM. Levodopa and dopamine analogs as DNA polymerase inhibition and antitumor agents in human melanoma. Cancer Res 1980;40:1414–8.
[24] Yamada I, Seki S, Ito S, Matsubara O, Kasuga T. The killing effect of 4-S-cysteaminylphenol, a newly synthesized melanin precursor, on B16 melanoma cell lines. Br J Cancer 1991;63:187–90.
[25] Hasegawa K, Ito S, Inoue S, Wakamatsu K, Ozeki H, Ishiguro I. Dihydroxy-1,4-benzothiazine-6,7-dione, the ultimate toxic metabolite of 4-S-cysteaminylphenol and 4-S-cysteaminylcatechol. Biochem Pharmacol 1997;53:1435–44.
[26] Denning TL, Takaishi H, Crowe SE, Boldogh I, Jevnikar A, Ernst PB. Oxidative stress induces the expression of Fas and Fas ligand and apoptosis in murine intestinal epithelial cells. Free Radic Biol Med 2002;33:1641–50.
[27] Circu ML, Aw TY. Reactive oxygen species, cellular redox systems, and apoptosis. Free Radic Biol Med 2010;48:749–62.
[28] Shellman YG, Howe WR, Miller LA, Goldstein NB, Pacheco TR, Mahajan RL, et al. Hyperthermia induces endoplasmic reticulum-mediated apoptosis in melanoma and non-melanoma skin cancer cells. J Invest Dermatol 2008;128: 949–56.
[29] Itoh K, Mochizuki M, Ishii Y, Ishii T, Shibata T, Kawamoto Y, et al. Transcription factor Nrf2 regulates inflammation by mediating the effect of 15-deoxy-$\Delta^{12,14}$-prostaglandin J_2. Mol Cell Biol 2004;24:36–45.
[30] Jian Z, Li K, Liu L, Zhang Y, Zhou Z, Li C, et al. Heme oxygenase-1 protects human melanocytes from H_2O_2-induced oxidative stress via the Nrf2-ARE pathway. J Invest Dermatol 2011;131:1420–7.
[31] Ito A, Tanaka K, Kondo K, Shinkai M, Honda H, Matsumoto K, et al. Tumor regression by combined immunotherapy and hyperthermia using magnetic nanoparticles in an experimental subcutaneous murine melanoma. Cancer Sci 2003;94:308–13.
[32] Suzuki M, Shinkai M, Honda H, Kobayashi T. Anticancer effect and immune induction by hyperthermia of malignant melanoma using magnetite cationic liposomes. Melanoma Res 2003;13:129–35.
[33] Sato A, Tamura Y, Sato N, Yamashita T, Takada T, Sato M, et al. Melanoma-targeted chemo-thermo-immuno (CTI)-therapy using N-propionyl-4-S-cysteaminylphenol-magnetite nanoparticles elicits CTL response via heat shock protein–peptide complex release. Cancer Sci 2010;101:1939–46.
[34] Bronte V, Apolloni E, Ronca R, Zamboni P, Overwijk WW, Surman DR, et al. Genetic vaccination with "self" tyrosinase-related protein 2 causes melanoma eradication but not vitiligo. Cancer Res 2000;60:253–8.
[35] Mendiratta SK, Thai G, Eslahi NK, Thull NM, Matar M, Bronte V, et al. Therapeutic tumor immunity induced by polyimmunization with melanoma antigens gp100 and TRP-2. Cancer Res 2001;61:859–63.
[36] Ji Q, Gondek D, Hurwitz AA. Provision of granulocyte–macrophage colony-stimulating factor converts an autoimmune response to a self-antigen into an antitumor response. J Immunol 2005;175:1456–63.
[37] Westerhof W, d'Ischia M. Vitiligo puzzle: the pieces fall in place. Pigment Cell Res 2007;20:345–59.
[38] Westerhof W, Manini P, Napolitano A, d'Ischia M. The haptenation theory of vitiligo and melanoma rejection: a close-up. Exp Dermatol 2011;20:92–6.

Cancer Science
The official journal of the Japanese Cancer Association JCA

SYT-SSX breakpoint peptide vaccines in patients with synovial sarcoma: A study from the Japanese Musculoskeletal Oncology Group[19]

Satoshi Kawaguchi,[1,18] Tomohide Tsukahara,[1,2] Kazunori Ida,[1,2] Shigeharu Kimura,[1,2] Masaki Murase,[1,2] Masanobu Kano,[1,2] Makoto Emori,[1,2] Satoshi Nagoya,[1] Mitsunori Kaya,[1] Toshihiko Torigoe,[2] Emiri Ueda,[2] Akari Takahashi,[2] Takeshi Ishii,[3] Shin-ichiro Tatezaki,[3] Junya Toguchida,[4] Hiroyuki Tsuchiya,[5] Toshihisa Osanai,[6] Takashi Sugita,[7] Hideshi Sugiura,[8] Makoto Ieguchi,[9] Koichiro Ihara,[10] Ken-ichiro Hamada,[11] Hiroshi Kakizaki,[12] Takeshi Morii,[13] Taketoshi Yasuda,[14] Taisuke Tanizawa,[15] Akira Ogose,[16] Hiroo Yabe,[17] Toshihiko Yamashita,[1] Noriyuki Sato[2] and Takuro Wada[1]

[1]Departments of Orthopaedic Surgery; [2]Pathology, Sapporo Medical University School of Medicine, Sapporo; [3]Division of Orthopaedic Surgery, Chiba Cancer Center Hospital, Chiba; [4]Department of Tissue Regeneration, Institute for Frontier Medical Sciences, Kyoto University, Kyoto; [5]Department of Orthopaedic Surgery, Kanazawa University, Kanazawa; [6]Department of Orthopaedic Surgery, Yamagata University, Yamagata; [7]Department of Orthopaedic Surgery, Hiroshima Prefectural Hospital, Hiroshima; [8]Department of Orthopaedic Surgery, Aichi Cancer Center Hospital, Nagoya; [9]Department of Orthopaedic Surgery, Osaka City University, Osaka; [10]Department of Orthopaedic Surgery, Kanmon Medical Center, Shimonoseki; [11]Department of Orthopaedic Surgery, Osaka Medical Center for Cancer and Cardiovascular Diseases, Osaka; [12]Department of Orthopaedic Surgery, Hirosaki National Hospital, Hirosaki; [13]Department of Orthopaedic Surgery, Kyorin University, Tokyo; [14]Department of Orthopaedic Surgery, Toyama University, Toyama; [15]Department of Orthopaedic Surgery, Cancer Instiute Hospital, Tokyo; [16]Department of Orthopaedic Surgery, Niigata University, Niigata; [17]Department of Orthopaedic Surgery, Keio University, Tokyo, Japan

(Received April 25, 2012/Revised June 7, 2012/Accepted June 10, 2012/Accepted manuscript online June 24, 2012/Article first published online August 7, 2012)

In the present study, we evaluated the safety and effectiveness of SYT-SSX-derived peptide vaccines in patients with advanced synovial sarcoma. A 9-mer peptide spanning the SYT-SSX fusion region (B peptide) and its HLA-A*2402 anchor substitute (K9I) were synthesized. In Protocols A1 and A2, vaccines with peptide alone were administered subcutaneously six times at 14-day intervals. The B peptide was used in Protocol A1, whereas the K9I peptide was used in Protocol A2. In Protocols B1 and B2, the peptide was mixed with incomplete Freund's adjuvant and then administered subcutaneously six times at 14-day intervals. In addition, interferon-α was injected subcutaneously on the same day and again 3 days after the vaccination. The B peptide and K9I peptide were used in Protocols B1 and B2, respectively. In total, 21 patients (12 men, nine women; mean age 43.6 years) were enrolled in the present study. Each patient had multiple metastatic lesions of the lung. Thirteen patients completed the six-injection vaccination schedule. One patient developed intracerebral hemorrhage after the second vaccination. Delayed-type hypersensitivity skin tests were negative in all patients. Nine patients showed a greater than twofold increase in the frequency of CTLs in tetramer analysis. Recognized disease progression occurred in all but one of the nine patients in Protocols A1 and A2. In contrast, half the 12 patients had stable disease during the vaccination period in Protocols B1 and B2. Of note, one patient showed transient shrinkage of a metastatic lesion. The response of the patients to the B protocols is encouraging and warrants further investigation. (*Cancer Sci* 2012; 103: 1625–1630)

Synovial sarcoma is a malignant tumor of soft tissue characterized by biphasic or monophasic histology, specific chromosomal translocation t(X;18), and its resultant *SYT-SSX* fusion genes.[1,2] Reported 5-year survival rates of patients with synovial sarcoma range from 64% to 77%.[3–7] In contrast, most metastatic or relapsed diseases remain incurable, indicating a need for new therapeutic options other than conventional surgery, radiotherapy, and chemotherapy.

Antigen-specific peptide immunotherapy is one such option.[8–12] Previously, we demonstrated that *SYT-SSX* fusion gene-derived peptides (wild type and agretope modified) are recognized by circulating $CD8^+$ T cells in HLA-$A24^+$ patients with synovial sarcoma and elicit human leukocyte antigen (HLA)-restricted, tumor-specific cytotoxic responses.[13,14] Subsequent to these preclinical studies, we started a pilot clinical trial with a wild-type SYT-SSX-derived peptide vaccine.[15] In the present study, we evaluated immunologic and clinical outcomes of the vaccination trials using an agretope-modified SYT-SSX peptide and a combination of the peptide vaccine with adjuvant and interferon (IFN)-α.

Materials and Methods

Eligibility. The study protocol was approved by the Clinical Institutional Ethical Review Board of the Medical Institute of Bioregulation, Sapporo Medical University, Sapporo, Japan. Eligible patients were those who: (i) had histologically and genetically confirmed unresectable synovial sarcoma (*SYT-SSX1* or *SYT-SSX2* positive); (ii) were HLA-A*2402 positive; (iii) were between 20 and 70 years of age; (iv) had Eastern Cooperative Oncology Group (ECOG) performance status between 0 and 3; and (v) provided informed consent. Exclusion criteria included: (i) prior chemotherapy, steroid therapy, or other immunotherapy within the previous 4 weeks; (ii) the presence of other cancers that may influence prognosis; (iii) immunodeficiency or a history of splenectomy; (iv) severe cardiac insufficiency, acute infection, or hematopoietic failure; (v) ongoing breast-feeding; and (vi) unsuitability for the trial based on the clinical judgment of the doctors involved.

Peptide. A 9-mer peptide (Peptide B: GYDQIMPKK) spanning the SYT-SSX fusion region and its HLA-A*2402 anchor substitute (Peptide K9I: GYDQIMPKI), in which lysine at position 9 was substituted to isoleucine, were synthesized under good manufacturing practice (GMP) conditions by Multiple Peptide Systems (San Diego, CA, USA). The identity of

[18]To whom correspondence should be addressed.
E-mail: kawaguch@sapmed.ac.jp
[19]This study has been registered with the UMIN Clinical Trials Registry (registration no.: UMIN 000001359).

doi: 10.1111/j.1349-7006.2012.02370.x

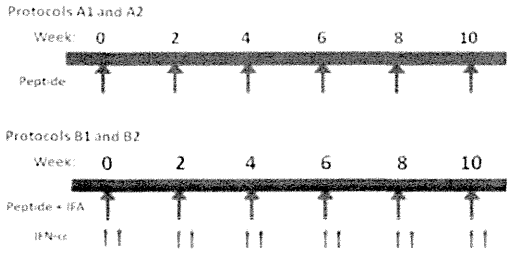

Fig. 1. Vaccination protocols. In Protocols A, vaccines with K9I peptide were administered subcutaneously six times at 14-day intervals. In Protocols B, a mixture of SYT-SSX B peptide and incomplete Freund's adjuvant (IFA) was administered subcutaneously six times at 14-day intervals. In addition, interferon (IFN)-α was injected on the same day as the vaccination and 3 days after the vaccination. The B peptide was used in Protocols A1 and B1, whereas the K9I peptide was used in Protocols A2 and B2.

the peptide was confirmed by mass spectral analysis, and it was shown to have >98% purity when assessed by HPLC. The peptides were delivered to us as sterile, freeze-dried white powders. They were dissolved in 1.0 mL physiological saline (Otsuka Pharmaceutical, Tokyo, Japan) and were stored at −80°C until just before use. The affinity of the peptides to HLA-A24 molecules and their antigenicity has been determined in previous studies.[13,14]

Vaccination schedule. Four protocols were used (Fig. 1). In Protocols A1 and A2, vaccines with the peptide alone (0.1 or 1 mg) were administered subcutaneously into the upper arm six times at 14-day intervals. The SYT-SSX B peptide (0.1 or 1 mg) was used in Protocol A1, as reported previously,[15] whereas the K9I peptide (1 mg) was used in Protocol A2. In Protocols B1 and B2, 1 mL peptide was mixed with 1 mL incomplete Freund's adjuvant (IFA, Montanide ISA 51; Seppic Inc., Fairfield, NJ, USA). The mixture was then administered subcutaneously into the upper arm six times at 14-day intervals. In addition, 3×10^6 U IFN-α (Sumiferon; Sumitomo Pharmaceuticals, Osaka, Japan) was injected subcutaneously into the upper arm on the same day together with the vaccination and again 3 days after vaccination. The B peptide (1 mg) was used in Protocol B1, whereas the K9I peptide (1 mg) was used in Protocol B2.

Delayed-type hypersensitivity skin test. A delayed-type hypersensitivity (DTH) skin test was performed at the time of each vaccination. The peptide (10 μg) solution in physiological saline (0.1 mL) and the physiological saline itself (0.1 mL) were separately injected intradermally into the forearm. A positive reaction was defined as the presence of erythema (diameter >4 mm) 48 h after injection.

Toxicity evaluation. Patients were examined closely for signs of toxicity during and after vaccination. Adverse events were recorded using the National Cancer Institute Common Terminology Criteria for Adverse Events v3.0 (CTCAE; http://ctep.cancer.gov/protocolDevelopment/electronic_applications/docs/ctcaev3.pdf).

Tetramer-based frequency analysis. The frequency of peptide-specific CTLs was determined by tetramer-based analysis. The HLA-A24/peptide tetramers (HLA-A24/K9I, HLA-A24/B and HLA-A24/HIV) were constructed as described previously.[13,14,16] The PBMCs were obtained prior to vaccination and then again 1 week after the first, third, and sixth vaccinations.

In Protocols A1, A2, and B2, cells were stained with phycoerythrin (PE)–Cy5-conjugated anti-CD8 antibody (eBioscience, San Diego, CA, USA), PE-conjugated HLA-A24/B tetramer or HLA-A24/K9I tetramer, and FITC-conjugated HLA-A24/HIV tetramer. The $CD8^+$ living cells were gated and cells labeled with the HLA-A24/B (or K9I) tetramer, but not the HLA-A24/HIV tetramer, were referred to as tetramer-positive cells (Fig. S1). Analysis of stained PBMCs was performed using a FACS Caliber (Becton Dickinson, San Jose, CA, USA) and CellQuest software (Becton Dickinson). The frequency of CTLs was calculated as the number of tetramer-positive cells/number of $CD8^+$ cells.[15]

In Protocol B1, cells were first stimulated by limited dilution/mixed lymphocyte peptide culture (LD/MLPC) in 96-well plates, as described previously.[16,17] Cells were stained with PE–Cy5-conjugated anti-CD8 antibody, PE-conjugated HLA-A24/K9I tetramer, and FITC-conjugated HLA-A24/HIV tetramer. Cells were analyzed by flow cytometry using FACS Caliber and CellQuest. The $CD8^+$ living cells were gated and cells labeled with the HLA-A24/K9I tetramer, but not the HLA-A24/HIV tetramer, were referred to as tetramer-positive cells. Wells containing tetramer-positive cells were referred to as tetramer-positive wells. The frequency of CTLs was calculated as follows (see Fig. S2): (number of tetramer-positive wells)/(total number of $CD8^+$ cells seeded).[16,17]

Evaluation of the clinical response. Physical and hematological examinations were performed before and after each vaccination. Tumor size was evaluated by computed tomography (CT) scans before treatment, after three vaccinations, and then at the end of the study period. A complete response (CR) was defined as the complete disappearance of all measurable disease. A partial response (PR) was defined as at least a 30% decrease in the sum of diameters of target lesions, taking as reference the baseline sum diameters. Progressive disease (PD) was defined as at least a 20% increase in the sum of diameters of target lesions, taking as reference the smallest sum on study or by the appearance of new lesions. Stable disease (SD) was defined as the absence of matched criteria for CR, PR, or PD.

Results

In all, 21 patients were enrolled in the present study (Table 1). The initial six patients (Protocol A1) reported previously[15] were included for reference. There were 12 men and nine women in the study, with a mean age of 43.6 years (range 21–69 years). Each patient had multiple metastatic lesions of the lung.

A six-injection vaccination schedule was completed in 13 patients. Seven patients discontinued the vaccination regimen because of rapid disease progression. One patient (Patient 16) developed intracerebral hemorrhage after the second vaccination and discontinued thereafter. This patient had been on anticoagulation therapy (warfarin, cirostazol, and limaprost) for more than 2 years following vascular reconstruction surgery. The international normalized ratio (INR) and platelet count at the time of the second vaccination in this patient were 2.01 and 197 000/μL, respectively. The patient had no history of hypertension or diabetes and blood pressure was 109/65 mmHg at the time of vaccination. The intracranial hemorrhage was treated conservatively. One patient each in Protocols A1 and A2 and all six patients in Protocols B1 and B2 experienced fever after vaccination. One patient (Patient 11) had erythema on the vaccine injection site (Fig. 2).

The DTH skin test was negative in all patients. Tetramer-based frequency analysis was performed in 19 patients. As indicated in Table 2 and shown in Figure 3, three patients (Patients 2, 4, and 6) in Protocol A1, one (Patient 7) in Protocol A2 and three (Patients 16, 17, and 18) in Protocol B2 exhibited a greater than twofold increase in the frequency of CTLs.

Recognized disease progression occurred in all but one (Patient 5) of the nine patients in Protocols A (A1 and A2) during the vaccination period (Table 1). In contrast, disease

doi: 10.1111/j.1349-7006.2012.02370.x

Table 1. Profiles of participants and clinical responses

	Age (years)	Gender	Location of the metastatic tumor	No. vaccination	Adverse events	Evaluation of CT images	Follow up (months)	Status
Protocol A1								
Patient 1	69	M	Bil. lungs	1	—	PD	1	DOD
Patient 2	32	M	Bil. lungs	3	—	PD	2	DOD
Patient 3	21	F	Bil. lungs	6	—	PD	5	DOD
Patient 4	21	M	Bil. lungs	6	—	PD	6	DOD
Patient 5	39	F	Bil. lungs	6	Fever	SD	12	DOD
Patient 6	26	M	Bil. lungs	4	—	PD	6	DOD
Protocol A2								
Patient 7	30	M	Bil. lungs, RP	6	Fever	PD	8	DOD
Patient 8	63	F	Bil. lungs	6	—	PD	8	DOD
Patient 9	28	M	Bil. lungs	2	—	PD	1	DOD
Protocol B1								
Patient 10	63	F	Bil. lungs	6	Fever	SD	10	DOD
Patient 11	28	F	Bil. lungs	6	Fever	SD	57	AWD
Patient 12	24	M	Bil. lungs	6	Fever	PD	14	DOD
Patient 13	60	M	Bil. lungs	6	Fever	SD	48	AWD
Patient 14	42	F	Bil. lungs	6	Fever	PD	7	DOD
Patient 15	36	M	Bil. lungs	4	Fever	PD	1	DOD
Protocol B2								
Patient 16	52	F	Bil. lungs	2	Fever, ICH	PD	3	DOD
Patient 17	66	M	Bil. lungs	6	Fever	SD	27	DOD
Patient 18	61	F	Unilat. lung	6	Fever	SD	16	AWD
Patient 19	57	M	Bil. lungs	2	Fever	PD	1	DOD
Patient 20	64	F	Bil. lungs	2	Fever	PD	1	DOD
Patient 21	34	M	Unilat. lung	6	Fever	SD	6	AWD

AWD, alive with disease; Bil., bilateral; DOD, death of the disease; ICH, intracerebral hemorrhage; NA, not available; PD, progressive disease; RP, retroperitoneual space; SD, stable disease; Unilat., unilateral.

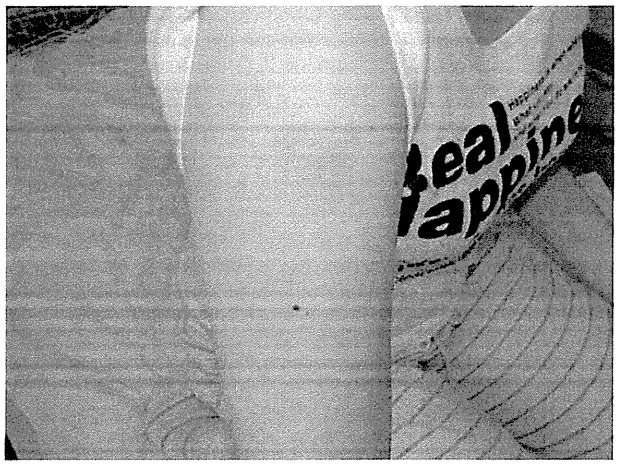

Fig. 2. Vaccination site in Patient 11. The patient received a vaccination in the right upper arm and erythema developed at the vaccination site.

progression was noted in only half of the 12 patients in Protocols B (B1 and B2; Fig. 4). The remaining six patients had stable disease during the vaccination period. Of these, one patient (Patient 17) exhibited transient shrinkage of a metastatic lesion (Fig. 5).

Discussion

In the present study, we evaluated the safety and effectiveness of SYT-SSX-derived peptide vaccines in 21 patients with

Table 2. HLA-A24/peptide tetramer analysis

	Before-vaccination	After 1st vaccination	After 3rd vaccination	After 6th vaccination
Protocol A1				
Patient 1	NA	NA	NA	NA
Patient 2	2	2	305	NA
Patient 3	42	49	52	62
Patient 4	6	41	36	47
Patient 5	50	52	9	3
Patient 6	2	15	8	NA
Protocol A2				
Patient 7	4	3	14	9
Patient 8	3	1	2	6
Patient 9	0	0	NA	NA
Protocol B1				
Patient 10	0	0	0.01	0
Patient 11	0.12	0.04	0.09	0.06
Patient 12	0.07	0.01	0.06	0.02
Patient 13	0.13	0.13	0.13	0.13
Patient 14	0.21	NA	NA	0.22
Patient 15	0.14	0.14	0.17	NA
Protocol B2				
Patient 16	0	27	NA	NA
Patient 17	8	1	25	34
Patient 18	7	24	13	39
Patient 19	NA	NA	NA	NA
Patient 20	16	25	NA	NA
Patient 21	24	22	18	11

For Protocols A1, A2, and B2, the data show the number of tetramer-positive $CD8^+$ cells in a population of 10 000 $CD8^+$ cells. For Protocol B1, the data show the number of tetramer-positive wells in a population of 10 000 $CD8^+$ cells. NA, not available.

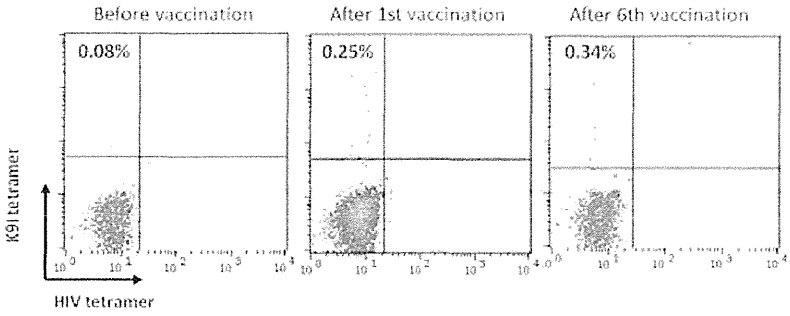

Fig. 3. Frequency of CTLs analyzed by HLA-A24/peptide tetramers in Patient 17.

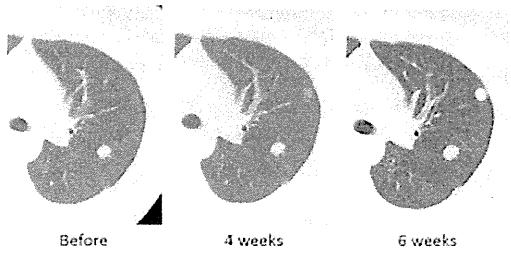

Fig. 4. Computed tomography scans of the lung in Patient 12 before vaccination on the day of the first vaccination and 4 and 6 weeks after the first vaccination. Growth of metastatic tumors was seen during the vaccination period.

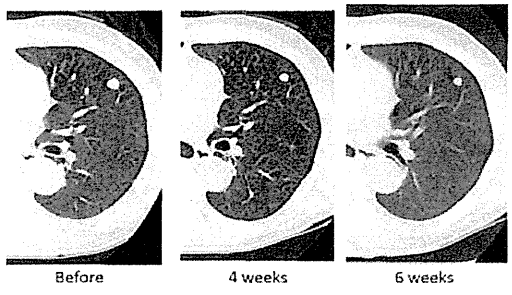

Fig. 5. Computed tomography scans of the lung in Patient 17 before vaccination on the day of the first vaccination and 4 and 6 weeks after the first vaccination. A decrease in the size of a metastatic tumor was seen during the first 6 weeks of the vaccination period.

advanced synovial sarcoma using four different protocols. Vaccines were administered safely in 20 patients. However, one patient in Protocol B2 (Patient 16; K9I peptide, IFA and IFN-α) developed intracerebral hemorrhage during the vaccination period. To our knowledge, such adverse events have not been reported previously in the literature of anticancer peptide vaccination trials. In contrast, there have been a few reported cases of intracerebral hemorrhage associated with IFN therapy.[18–20] These patients were either long-term users of IFN[18,19] or had comorbidities of hypertension or diabetes.[20] Interferon is known to cause thrombocytopenia.[21,22] Nevertheless, Patient 16 was not a long-term user of IFN and did not have any of those complications or thrombocytopenia. However, the patient had been on anticoagulants for more than 2 years. Intracranial hemorrhage is a known complication of anticoagulant therapy, with an estimated annual incidence in the US of nearly 3000.[23] In addition, approximately half the cases of anticoagulant-associated intracranial hemorrhage occurred within or below the INR therapeutic range (2.0–3.0).[24] It is therefore more likely that the intracranial hemorrhage in Patient 16 was associated with anticoagulants rather than the peptide vaccine or IFN.

With regard to the efficacy of the protocols, the tumors showed dormancy during the vaccination period in six of 12 patients (50%) in Protocols B1 and B2, including one patient exhibiting transient shrinkage of a metastatic lesion. In contrast, only one (11%) of the nine patients who received the peptide vaccine by itself showed such tumor dormancy. In addition, a greater number of patients completed the six-injection vaccination regimen in Protocol B (80%) than in the protocols with the peptide itself. These findings indicate that the adjuvant activity of IFA and IFN-α enhance the antitumor effects of the peptide vaccine. Interferon-α is a cytokine with various biological activities. In a murine model with antimelanoma peptide vaccination, administration of IFN-α enhanced antigen presentation and promoted the effector function of peptide-specific CTLs.[25] This was attributed to the induction by IFN-α of dendritic cell maturation and expression of HLA molecules on tumor cells. Such adjuvant activities of IFN-α have also been seen in clinical vaccination trials.[26–28] In contrast, IFN-α itself has direct antitumor properties.[29] Brodowicz *et al.*[30] reported inhibitory effects of IFN-α on the proliferation of a synovial sarcoma cell line *in vitro*. However, no clinical studies have addressed direct the antitumor effects of IFN-α on synovial sarcoma. Unless we evaluate a protocol with IFN-α by itself or a protocol with only IFA and IFN-α, it remains unclear whether the clinical responses seen in patients in Protocol B are due to the effects of IFA and IFN-α or to the synergistic effects of the peptide vaccine, IFA, and IFN-α.

The K9I peptide is an agretope-modified peptide in which an HLA-A24 anchor residue of the B peptide (lysine at position 9) is substituted to isoleucine.[14] In a previous study,[14] this substitution enhanced the affinity for HLA-A24 molecules and improved the capacity of the peptide to induce synovial sarcoma-specific CTLs *in vitro*. In the present study, a greater than twofold increase in the frequency of CTLs was seen in three patients (25%) in Protocols A1 and B1 (B peptide) and in four patients (44%) in Protocols A2 and B2 (K9I peptide). Although the percentage of patients exhibiting tumor dormancy was 33% in both the B peptide and K9I peptide groups, tumor shrinkage was observed only in a patient treated with the K9I peptide (Protocol B2). These findings may reflect higher immunogenic properties of the K9I peptide than the B peptide. Indeed, an agretope-modified peptide has been used in a mixture with wild-type peptides in bcr-abl fusion gene peptide vaccines for CML.[31]

Analysis of peripheral blood lymphocytes using HLA-A24/peptide tetramers revealed a greater than twofold increase in the peptide-specific CTL frequency in seven patients. However, the immune responses had no relevance to the clinical responses. One possible explanation for this is that analysis of peripheral lymphocytes does not properly reflect the immunological environment at the tumor site. It remains unknown how many vaccine-specific CTLs were recruited into the tumor site. In addition, the cytotoxic function of CTLs may be suppressed

doi: 10.1111/j.1349-7006.2012.02370.x

in the tumor site by certain mechanisms, such as downregulation of Class I molecules and immunosuppressive effects of regulatory T cells. A combination of tetramer analysis with other monitoring assays, such as enzyme-linked immunospot (ELISPOT), may provide more precise information about the immunological status of patients.

Vaccination trials of fusion gene-derived peptides have been reported with EWS-FLI1 in Ewing's sarcoma,[32] PAX3-FKHR in alveolar rhabdomyosarcoma,[32] and BCR-ABL in CML.[31,33–36] Tumor regression was seen more frequently in studies with CML than in those with sarcomas. One reason for such differences in outcome is the additional use of Class II peptide vaccines in the CML studies.[10,11,36,37] Another possible explanation is the introduction of a highly effective therapy for CML, such as the administration of imatinib, which enables a reduction of the tumor mass prior to initiation of peptide vaccination.

Apart from direct vaccinations of peptides into patients, SYT-SSX-derived peptides have been used to stimulate dendritic cells in adoptive immunotherapy for patients with synovial sarcoma.[38,39] More recently, the T cell receptor was engineered to recognize an NY-ESO-1-derived peptide and was transduced into autologous T cells. Adoptive immunotherapy using these genetically engineered T cells conferred objective clinical responses (PR) in four of six patients with synovial sarcoma.[40] In contrast with adoptive immunotherapy, peptide vaccination would suit a setting with small tumor burden or an adjuvant setting. In this regard, an HER2-derived peptide vaccine has been used to prevent recurrence from breast cancer in clinical trials.[41,42]

In conclusion, the present study is the first clinical trial of SYT-SSX breakpoint peptide vaccines combined with IFA and IFN-α. The response of patients to Protocols B is encouraging and warrants further investigation, ideally in an adjuvant setting.

Acknowledgments

This work was supported by Grants-in-Aid from the Ministry of Education, Culture, Sports, Science and Technology of Japan (16209013, 17016061 and 15659097 to NS; 20390403 to TW; 22689041 to TT), the Japan Science and Technology Agency (to NS), from the Ministry of Health, Labor and Welfare (to NS and TW), National Cancer Center Research and Development Fund (23-A-10 and 23-A-44 to TW), the Japan Orthopaedics and Traumatology Foundation (198 to TT), and the Akiyama Life Science Foundation (Syorei No. 7, 2010 to TT).

Disclosure Statement

The authors declare no conflicts of interest.

References

1 Eilber FC, Dry SM. Diagnosis and management of synovial sarcoma. *J Surg Oncol* 2008; **97**: 314–20.
2 Fisher C. Soft tissue sarcomas with non-EWS translocations: molecular genetic features and pathologic and clinical correlations. *Virchows Arch* 2010; **456**: 153–66.
3 Ferrari A, Bisogno G, Alaggio R *et al.* Synovial sarcoma of children and adolescents: the prognostic role of axial sites. *Eur J Cancer* 2008; **44**: 1202–9.
4 Italiano A, Penel N, Robin YM *et al.* Neo/adjuvant chemotherapy does not improve outcome in resected primary synovial sarcoma: a study of the French Sarcoma Group. *Ann Oncol* 2009; **20**: 425–30.
5 Palmerini E, Staals EL, Alberghini M *et al.* Synovial sarcoma: retrospective analysis of 250 patients treated at a single institution. *Cancer* 2009; **115**: 2988–98.
6 Sultan I, Rodriguez-Galindo C, Saab R, Yasir S, Casanova M, Ferrari A. Comparing children and adults with synovial sarcoma in the Surveillance, Epidemiology, and End Results program, 1983 to 2005: an analysis of 1268 patients. *Cancer* 2009; **115**: 3537–47.
7 Brennan B, Stevens M, Kelsey A, Stiller CA. Synovial sarcoma in childhood and adolescence: a retrospective series of 77 patients registered by the Children's Cancer and Leukaemia Group between 1991 and 2006. *Pediatr Blood Cancer* 2010; **55**: 85–90.
8 Melief CJ, van der Burg SH. Immunotherapy of established (pre)malignant disease by synthetic long peptide vaccines. *Nat Rev Cancer* 2008; **8**: 351–60.
9 Finn OJ. Cancer immunology. *N Engl J Med* 2008; **358**: 2704–15.
10 Khazaie K, Bonertz A, Beckhove P. Current developments with peptide-based human tumor vaccines. *Curr Opin Oncol* 2009; **21**: 524–30.
11 Perez SA, von Hofe E, Kallinteris NL *et al.* A new era in anticancer peptide vaccines. *Cancer* 2010; **116**: 2071–80.
12 Pollack SM, Loggers ET, Rodler ET, Yee C, Jones RL. Immune-based therapies for sarcoma. *Sarcoma* 2011; **2011**: 438940.
13 Sato Y, Nabeta Y, Tsukahara T *et al.* Detection and induction of CTLs specific for SYT-SSX-derived peptides in HLA-A24(+) patients with synovial sarcoma. *J Immunol* 2002; **169**: 1611–8.
14 Ida K, Kawaguchi S, Sato Y *et al.* Crisscross CTL induction by SYT-SSX junction peptide and its HLA-A*2402 anchor substitute. *J Immunol* 2004; **173**: 1436–43.
15 Kawaguchi S, Wada T, Ida K *et al.* Phase I vaccination trial of SYT-SSX junction peptide in patients with disseminated synovial sarcoma. *J Transl Med* 2005; **3**: 1.
16 Tsukahara T, Kawaguchi S, Torigoe T *et al.* Prognostic impact and immunogenicity of a novel osteosarcoma antigen, papillomavirus binding factor, in patients with osteosarcoma. *Cancer Sci* 2008; **99**: 368–75.
17 Tsukahara T, Kawaguchi S, Torigoe T *et al.* HLA-A*0201-restricted CTL epitope of a novel osteosarcoma antigen, papillomavirus binding factor. *J Transl Med* 2009; **7**: 44.
18 Bailly F, Mattei A, SiAhmed SN, Trepo C. Uncommon side-effects of interferon. *J Viral Hepat* 1997; **4** (Suppl 1): 89–94.
19 Niederwieser G, Bonelli RM, Kammerhuber F, Reisecker F, Koltringer P. Intracerebral haemorrhage under interferon-beta therapy. *Eur J Neurol* 2001; **8**: 363–4.
20 Nishiofuku M, Tsujimoto T, Matsumura Y *et al.* Intracerebral hemorrhage in a patient receiving combination therapy of pegylated interferon alpha-2b and ribavirin for chronic hepatitis C. *Intern Med* 2006; **45**: 483–4.
21 Dourakis SP, Deutsch M, Hadziyannis SJ. Immune thrombocytopenia and alpha-interferon therapy. *J Hepatol* 1996; **25**: 972–5.
22 Yamane A, Nakamura T, Suzuki H *et al.* Interferon-alpha 2b-induced thrombocytopenia is caused by inhibition of platelet production but not proliferation and endomitosis in human megakaryocytes. *Blood* 2008; **112**: 542–50.
23 Cervera A, Amaro S, Chamorro A. Oral anticoagulant-associated intracerebral hemorrhage. *J Neurol* 2012; **259**: 212–24.
24 Mantha S, Pianka AM, Tsapatsaris N. Determinants of intracranial hemorrhage incidence in patients on oral anticoagulation followed at the Lahey clinic. *J Thromb Thrombolysis* 2011; **32**: 334–42.
25 Sikora AG, Jaffarzad N, Hailemichael Y *et al.* IFN-alpha enhances peptide vaccine-induced $CD8^+$ T cell numbers, effector function, and antitumor activity. *J Immunol* 2009; **182**: 7398–407.
26 Smith JW II, Walker EB, Fox BA *et al.* Adjuvant immunization of HLA-A2-positive melanoma patients with a modified gp100 peptide induces peptide-specific $CD8^+$ T-cell responses. *J Clin Oncol* 2003; **21**: 1562–73.
27 Di Pucchio T, Pilla L, Capone I *et al.* Immunization of stage IV melanoma patients with Melan-A/MART-1 and gp100 peptides plus IFN-alpha results in the activation of specific CD8(+) T cells and monocyte/dendritic cell precursors. *Cancer Res* 2006; **66**: 4943–51.
28 Amato RJ, Shingler W, Goonewardena M *et al.* Vaccination of renal cell cancer patients with modified vaccinia Ankara delivering the tumor antigen 5T4 (TroVax) alone or administered in combination with interferon-alpha (IFN-alpha): a phase 2 trial. *J Immunother* 2009; **32**: 765–72.
29 Whelan J, Patterson D, Perisoglou M *et al.* The role of interferons in the treatment of osteosarcoma. *Pediatr Blood Cancer* 2010; **54**: 350–4.
30 Brodowicz T, Wiltschke C, Kandioler-Eckersberger D *et al.* Inhibition of proliferation and induction of apoptosis in soft tissue sarcoma cells by interferon-alpha and retinoids. *Br J Cancer* 1999; **80**: 1350–8.
31 Jain N, Reuben JM, Kantarjian H *et al.* Synthetic tumor-specific breakpoint peptide vaccine in patients with chronic myeloid leukemia and minimal residual disease: a phase 2 trial. *Cancer* 2009; **115**: 3924–34.
32 Dagher R, Long LM, Read EJ *et al.* Pilot trial of tumor-specific peptide vaccination and continuous infusion interleukin-2 in patients with recurrent

Ewing sarcoma and alveolar rhabdomyosarcoma: an inter-institute NIH study. *Med Pediatr Oncol* 2002; **38**: 158–64.
33 Cathcart K, Pinilla-Ibarz J, Korontsvit T *et al.* A multivalent bcr-abl fusion peptide vaccination trial in patients with chronic myeloid leukemia. *Blood* 2004; **103**: 1037–42.
34 Bocchia M, Gentili S, Abruzzese E *et al.* Effect of a p210 multipeptide vaccine associated with imatinib or interferon in patients with chronic myeloid leukaemia and persistent residual disease: a multicentre observational trial. *Lancet* 2005; **365**: 657–62.
35 Rojas JM, Knight K, Wang L, Clark RE. Clinical evaluation of BCR-ABL peptide immunisation in chronic myeloid leukaemia: results of the EPIC study. *Leukemia* 2007; **21**: 2287–95.
36 Bocchia M, Defina M, Aprile L *et al.* Complete molecular response in CML after p210 BCR-ABL1-derived peptide vaccination. *Nat Rev Clin Oncol* 2010; **7**: 600–3.
37 Kanodia S, Kast WM. Peptide-based vaccines for cancer: realizing their potential. *Expert Rev Vaccines* 2008; **7**: 1533–45.
38 Matsuzaki A, Suminoe A, Hattori H, Hoshina T, Hara T. Immunotherapy with autologous dendritic cells and tumor-specific synthetic peptides for synovial sarcoma. *J Pediatr Hematol Oncol* 2002; **24**: 220–3.
39 Suminoe A, Matsuzaki A, Hattori H, Koga Y, Hara T. Immunotherapy with autologous dendritic cells and tumor antigens for children with refractory malignant solid tumors. *Pediatr Transplant* 2009; **13**: 746–53.
40 Robbins PF, Morgan RA, Feldman SA *et al.* Tumor regression in patients with metastatic synovial cell sarcoma and melanoma using genetically engineered lymphocytes reactive with NY-ESO-1. *J Clin Oncol* 2011; **29**: 917–24.
41 Holmes JP, Clifton GT, Patil R *et al.* Use of booster inoculations to sustain the clinical effect of an adjuvant breast cancer vaccine: from US Military Cancer Institute Clinical Trials Group Study I-01 and I-02. *Cancer* 2011; **117**: 463–71.
42 Mittendorf EA, Clifton GT, Holmes JP *et al.* Clinical trial results of the HER-2/neu (E75) vaccine to prevent breast cancer recurrence in high-risk patients: from US Military Cancer Institute Clinical Trials Group Study I-01 and I-02. *Cancer* 2012; **118**: 2594–602.

Supporting Information

Additional Supporting Information may be found in the online version of this article:

Fig. S1. Data acquisition and sequential gating (Protocols A1, A2 and B2).

Fig. S2. Limited dilution/mixed lymphocyte peptide culture (Protocol B1).

Please note: Wiley-Blackwell are not responsible for the content or functionality of any supporting materials supplied by the authors. Any queries (other than missing material) should be directed to the corresponding author for the article.

doi: 10.1111/j.1349-7006.2012.02370.x

Human Endoplasmic Reticulum Oxidoreductin 1-Like α (hERO1-L α) のMHC class I分子発現制御と癌免疫療法に対する効果予測因子としての可能性

久木田和晴[*1] 田村 保明[*2] 奥谷 浩一[*1] 斎藤 慶太[*1] 九冨 五郎[*1]
佐藤 昇志[*2] 平田 公一[*1]

〔*Jpn J Cancer Chemother* 39(12): 1800-1802, *November*, 2012〕

Human Endoplasmic Reticulum Oxidoreductin 1-Like α Regulates Immune Response of Cancer Cells Via Modulation of Major Histocompatibility Complex Class I Expression and Oxidation: Kazuharu Kukita[*1], Yasuaki Tamura[*2], Koichi Oku-ya[*1], Keita Saito[*1], Goro Kutomi[*1], Noriyuki Sato[*2] and Koichi Hirata[*1] (*[1]*First Dept. of Surgery, and* *[2]*First Dept. of Pathology, Sapporo Medical University*)

Summary

The protein human endoplasmic reticulum oxidoreductin 1-like α (hERO1-L α) is a hypoxia-inducible endoplasmic reticulum resident oxidase that regulates the redox state of various proteins via protein disulfide isomerase. The major histocompatibility complex (MHC) class I molecule contains intramolecular disulfide bonds. hERO1-L α is expressed within normoxic cells at very low levels, but may be induced in hypoxic cells such as tumor cells in response to low oxygen availability. We therefore examined whether hERO1-L α affects the oxidation state and expression level of MHC class I in the colon cancer cell line SW480. We generated SW480 cells in which hERO1-L α was overexpressed or knocked down. The surface expression of MHC class I molecule was upregulated in the hERO1-L α-overexpressing SW480 cells and downregulated in the hERO1-L α-knockdown SW480 cells. Moreover, the oxidized form of MHC class I was increased in the hERO1-L α-overexpressing SW480 cells, and the hERO1-L α-knockdown SW480 cells exhibited an impaired response to cytotoxic T lymphocytes. These data suggest that hERO1-L α regulates immune response via modulation of MHC class I expression and oxidation, and that hERO1-L α may act as a new predictive factor for cancer immunotherapy. **Key words:** hERO1-L α, MHC class I

要旨 癌免疫療法は，癌に対する新たな治療法として注目されているが，その効果は未だ十分といえず，同療法に対する効果予測因子も確定的なものがないのが現状である。癌免疫療法ではMHC class I分子の発現制御が重要な因子であり，MHC class I分子の安定的な発現にはS-S結合形成が必須である。そこでわれわれは，種々の蛋白質のS-S結合形成を担うhuman endoplasmic reticulum oxidoreductin 1-like α (hERO1-L α) に着目し，MHC class I分子発現との関連性を検討した。大腸癌細胞株のhERO1-L α過剰発現株にて，MHC class I分子の細胞表面への発現増加を認めた。一方，hERO1-L α knockdown細胞株では細胞表面上に発現するMHC class I分子が低下し，その結果癌特異的T細胞応答が減弱した。このようにhERO1-L αはMHC class I分子の発現および腫瘍免疫応答に重要な役割を担っており，癌免疫療法の効果予測因子となる可能性がある。

はじめに

癌免疫療法は悪性腫瘍に対する新たな治療方法として広がりをみせている。一部劇的な効果を認めるものの，抗腫瘍効果がまったくみられない症例も少なくない。癌免疫療法は，方法により能動免疫法と受動免疫法に分けられるが，当教室では能動免疫法である癌ワクチン療法に注目し，癌ワクチンとして同定した抗原分子を用いた臨床試験を行い一定の成果を上げているが，満足すべきものと断言すべきではない[1]。

癌ワクチン療法は，癌細胞のMHC class I分子により提示された癌特異的抗原peptideを認識する細胞傷害性

[*1] 札幌医科大学・第一外科
[*2] 同 ・第一病理

連絡先: 〒060-8556 北海道札幌市中央区南1条西16丁目 札幌医科大学・第一外科
久木田和晴

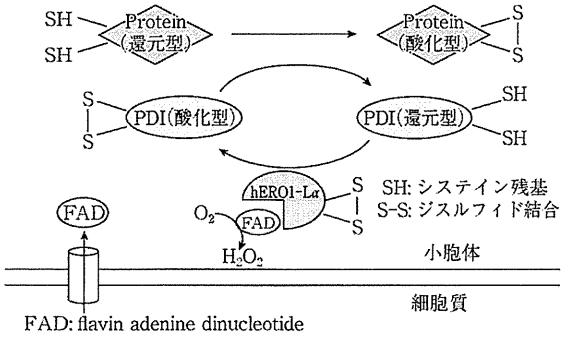

図 1　hERO1-L α-PDI による蛋白質の酸化・folding（ジスルフィド結合付加）

T リンパ球（CTL）を誘導することを目的としている。そのため MHC class I 分子の発現制御が，癌ワクチン療法の有効性を決定する重要なファクターの一つであることに疑いはない。また，癌細胞における MHC class I 分子の発現低下は癌ワクチン療法抵抗性の一因と考えられる。癌ワクチン療法の効果予測因子として確定的なものがないのが現状であるが，腫瘍細胞における MHC class I 分子の発現や，peptide の loading にかかわる分子が新たな癌ワクチン療法の効果予測因子となる可能性がある。

I.　hERO1-L α と MHC class I 分子の立体構造

hERO1-L α は，小胞体内に存在する酸化酵素で低酸素環境などにより発現が誘導されることが知られている。同分子は，蛋白質ジスルフィドイソメラーゼ（PDI）を酸化するが，この酸化型 PDI が対象となる蛋白質のシステイン残基対を酸化し，ジスルフィド結合（S-S 結合）を付加することにより，蛋白質の folding，品質管理に関与すると報告されている（図 1）。近年その立体構造や，hERO1-L α-PDI の詳細な分子間相互作用が解明されてきている[2-4]。

一方，MHC class I 分子内には三つの S-S 結合が存在しており，その立体構造形成・維持にたいへん重要な役割を果たしている。特に α2 ドメインに存在する S-S 結合が，peptide-binding groove の形成に必須であるとされ，MHC class I 分子が正しい立体構造をとり，抗原 peptide を乗せた状態で細胞表面へと発現するためには，小胞体内における酸化反応による S-S 結合が必要と考えられる。

小胞体内における MHC class I 分子の品質管理には，peptide-loading complex（PLC）と呼ばれる蛋白複合体が重要であるといわれるが，近年，PDI が PLC のメンバーであると報告され[5]，さらに PDI が MHC class I 分子の早期の folding に必要であると報告された[6]。

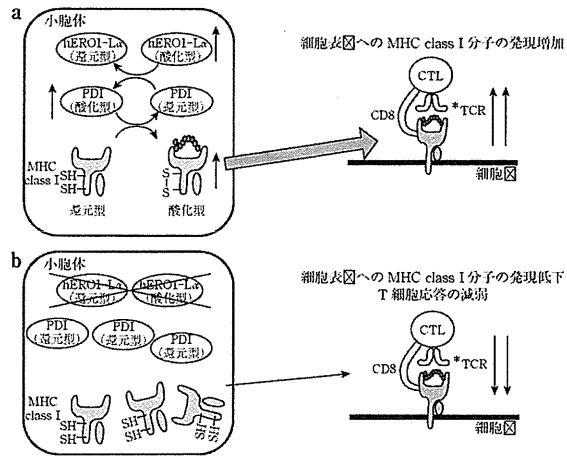

図 2　hERO1-L α の過剰発現による MHC class I 分子の発現増加と knockdown による MHC class I 分子の発現低下および T 細胞応答の減弱
*TCR: T cell receptor
a: hERO1-L α を過剰発現させると酸化型 PDI，酸化型（安定型）MHC class I 分子が増加し，細胞表面への MHC class I 分子の発現が増加する。
b: hERO1-L α を knockdown すると，還元型 PDI が増加し，細胞表面への MHC class I 分子の発現が低下，T 細胞応答が減弱する。

II.　腫瘍細胞における hERO1-L α の発現と MHC class I 分子発現制御

hERO1-L α の発現を RT-PCR にて検討したところ，正常組織と比較し，腫瘍細胞，特に大腸癌細胞株や膵癌細胞株において高発現していた。また，正常組織および癌組織を hERO1-L α に対する抗体を用いて免疫染色を行ったところ，正常組織ではその発現をまったく認めなかったが，癌組織においては高い陽性率を示した。また，種々の癌細胞株を低酸素培養（1% O_2）すると，PDI の発現は不変であったが，hERO1-L α が発現誘導されることを確認した。すなわち，hERO1-L α は癌腫や症例によって程度の差があるものの，癌化に伴う低酸素環境によって発現が誘導される可能性が考えられる。前述した hERO1-L α の機能と，MHC class I 分子の立体構造および細胞表面への発現の機序を考慮すれば，腫瘍組織における MHC class I 分子の発現と腫瘍免疫応答に hERO1-L α が重要な役割を果たしている可能性があると考えられ，さらに検討を進めた。

細胞内における hERO1-L α との会合分子を検討したところ，hERO1-L α は PDI，MHC class I 分子と分子会合していることが確認された。さらに，大腸癌細胞株（SW480）の hERO1-L α 過剰発現株および knockdown 細胞株を樹立し，MHC class I 分子の発現を検討した。過剰発現株において，S-S 結合を有した安定型の MHC

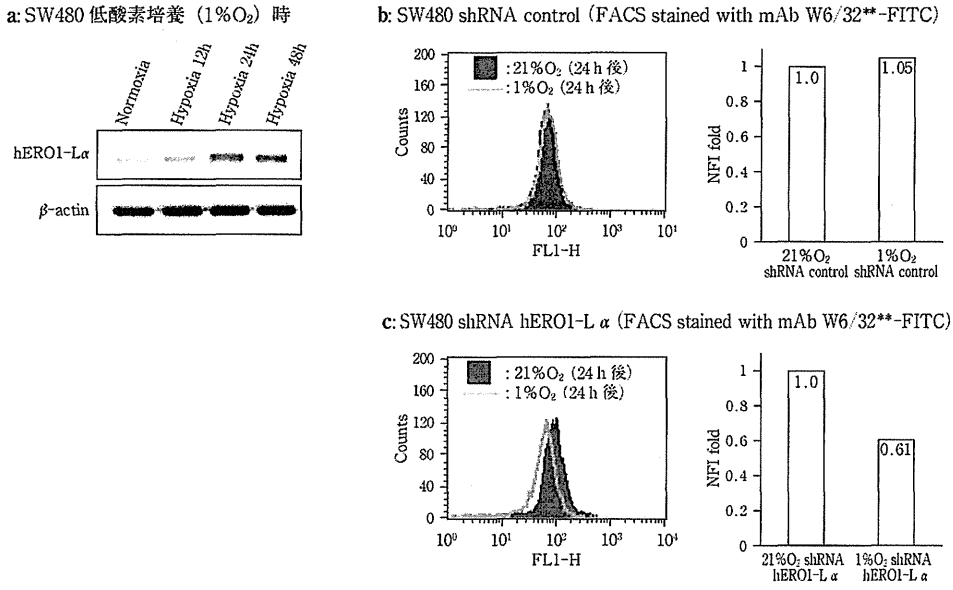

図 3 低酸素培養における hERO1-L α の誘導と hERO1-L α knockdown による MHC class I 分子の発現低下
a: 低酸素環境（1% O_2）にて SW480 細胞を培養すると hERO1-L α の発現が誘導される。
b, c: shRNA を用い hERO1-L α を knockdown すると，低酸素環境下で MHC class I 分子の細胞表面への発現が低下するが，control 群では不変であった。
**W6/32: anti-MHC class I

class I 分子の増加および細胞表面の発現増加を認め，knockdown 細胞株にて MHC class I 蛋白質が減少，細胞表面上に発現する MHC class I 分子も低下した。このような MHC class I 分子の発現低下により有意に T 細胞応答が減弱した（図 2）。SW480 を低酸素環境下（1% O_2）にて培養すると，WT では hERO1-L α の発現が誘導され，細胞表面への MHC class I 分子の発現が維持されていたが，hERO1-L α の knockdown 細胞株においては，MHC class I 分子の発現が低下した（図 3）。

ま と め

hERO1-L α は MHC class I 分子内の S-S 結合形成を制御し，その品質管理および発現制御を行っていることを示した。低酸素環境下での hERO1-L α 発現増強は，癌の特徴的な細胞周囲環境である低酸素環境下における MHC class I 分子の発現維持に寄与していると考えられる。さらに hERO1-L α は，S-S 結合形成による MHC class I 分子の立体構造形成のみならず，peptide の loading にも関与している可能性があり，検討中である。

以上より，hERO1-L α が高発現した癌腫，症例では，hERO1-L α が誘導されていないものと比較し，high-affinity peptide を乗せた質の高い MHC class I 分子の発現が維持され，peptide 特異的 CTL との高い反応性を示す可能性がある。将来的な癌ワクチン療法の効果予測因子としての応用も視野に入れ，さらなる検討を進めたい。

文 献

1) Tsuruma T, Iwayama Y, Ohmura T, *et al*: Clinical and immunological evaluation of anti-apoptosis protein, survivin-derived peptide vaccine in phase I clinical study for patients with advanced or recurrent breast cancer. *J Transl Med* **6**: 24, 2008.
2) Appenzeller-Herzog C, Riemer J, Zito E, *et al*: Disulphide production by Ero1 α-PDI relay is rapid and effectively regulated. *EMBO J* **29**(19): 3318-3329, 2010.
3) Inaba K, Masui S, Iida H, *et al*: Crystal structures of human Ero1 α reveal the mechanisms of regulated and targeted oxidation of PDI. *EMBO J* **29**(19): 3330-3343, 2010.
4) Araki K and Nagata K: Functional *in vitro* analysis of the ERO1 protein and protein-disulfide isomerase pathway. *J Biol Chem* **286**(37): 32705-32712, 2011.
5) Park B, Lee S, Kim E, *et al*: Redox regulation facilitates optimal peptide selection by MHC class I during antigen processing. *Cell* **127**(2): 369-382, 2006.
6) Kang K, Park B, Oh C, *et al*: A role for protein disulfide isomerase in the early folding and assembly of MHC class I molecules. *Antioxid Redox Signal* **11**(10): 2553-2561, 2009.

本論文の要旨は，第 70 回日本癌学会学術総会，第 33 回癌免疫外科研究会（奨励賞受賞論文）において発表した。実際のデータについては英文誌への論文投稿予定のため，データの詳細は図示にて代用させて頂いた。

Cancer Science
The official journal of the Japanese Cancer Association JCA

Anti-angiogenesis effect of 3′-sulfoquinovosyl-1′-monoacylglycerol via upregulation of thrombospondin 1

Kayo Matsuki,[1] Atsushi Tanabe,[2] Ayumi Hongo,[2] Fumio Sugawara,[3] Kengo Sakaguchi,[3] Nobuaki Takahashi,[1] Noriyuki Sato[1] and Hiroeki Sahara[1,2,4]

[1]Department of Pathology, Sapporo Medical University School of Medicine, Sapporo; [2]Laboratory of Biology, Azabu University School of Veterinary Medicine, Sagamihara; [3]Genome and Drug Research Center, Tokyo University of Science, Chiba, Japan

(Received January 12, 2012/Revised May 9, 2012/Accepted May 11, 2012/Accepted manuscript online May 16, 2012/Article first published online June 20, 2012)

We previously reported that 3′-sulfoquinovosyl-1′-monoacylglycerol (SQMG) effectively suppresses the growth of solid tumors, likely via its anti-angiogenic activity. To investigate how SQMG affects angiogenesis, we performed DNA microarray analysis and quantitative real-time polymerase chain reaction. Consequently, upregulation of thrombospondin 1 (TSP-1) in SQMG-treated tumors *in vitro* and *in vivo* was confirmed. To address the mechanisms of TSP-1 upregulation by SQMG, we established stable TSP-1-knockdown transformants (TSP1-KT) by short hairpin RNA induction and performed reporter assay and *in vivo* assessment of anti-tumor assay. On the reporter assay, transcriptional upregulation of TSP-1 in TSP1-KT could not be induced by SQMG, thus suggesting that TSP-1 upregulation by SQMG occurred via TSP-1 molecule. In addition, growth of TSP1-KT xenografted tumors *in vivo* was not inhibited by SQMG, thus suggesting that anti-angiogenesis via TSP-1 upregulation induced by SQMG did not occur, as the SQMG target molecule TSP-1 was knocked down in TSP1-KT transformants. These data provide that SQMG is a promising candidate for the treatment of tumor-induced angiogenesis via TSP-1 upregulation. (*Cancer Sci* 2012; 103: 1546–1552)

Angiogenesis, the formation of new blood vessels, is a fundamental process that is necessary for normal embryonic development and is also involved in the development of pathological conditions such as cancer.[1,2] Its importance in solid tumor growth and metastasis has been widely recognized by multiple studies.[2] A major pathway in tumor angiogenesis involves the vascular endothelial growth factor (VEGF) family of proteins and receptors.[3,4] Anti-angiogenic treatments are promising therapies for the treatment of cancer: for example, agents such as anti-VEGF antibodies that inhibit VEGF receptor tyrosine kinase and result in effective inhibition of solid tumor growth *in vivo* have been reported.[5,6]

Endogenous angiogenesis through VEGF/VEGF-receptor signaling is regulated by thrombospondin 1 (TSP-1). Expression of TSP-1 leads to the inhibition of angiogenic responses such as endothelial proliferation.[7–9] In addition, TSP-1 is involved in several other anti-angiogenic responses, such as inhibition of VEGF-stimulated VEGF receptor-2 (VEGFR-2) signaling[10,11] and VEGF trapping by its heparin sulfate proteoglycan domain.[12]

We previously reported that the growth of human adenocarcinoma tumors treated with 3′-sulfoquinovosyl-1′-monoacylglycerol (SQMG) was inhibited, and that these tumors showed extensive hemorrhagic necrosis on histopathological examination.[13,14] We also confirmed that only some tumor cell lines were sensitive to SQMG, and that angiogenesis was reduced *in vivo* in SQMG-sensitive tumors, but not in SQMG-resistant tumors.[15] Moreover, although a significant difference in *VEGF* gene expression was not detected in either SQMG-sensitive or SQMG-resistant tumors, significant downregulation of *Tie2* gene expression was observed in all of SQMG-sensitive tumors when compared with controls, but this downregulation was not observed in SQMG-resistant tumors.[15] These data suggest that the anti-tumor effects of SQMG can be attributed to the inhibition of angiogenesis.

Regardless of whether tumors are SQMG sensitive or resistant, the induced blood vessels are considered to be biologically similar. However, differences in the amount of *Tie2* gene expression in the endothelial cells are observed. Therefore, further investigation is necessary to understand the mechanisms underlying the anti-angiogenic effects of SQMG. In this study, we confirmed that SQMG treatment *in vitro* and *in vivo* results in the upregulation of the *TSP-1* gene in SQMG-sensitive tumors, but not in SQMG-resistant tumors, and that the effects of SQMG are nullified in TSP-1 knockdown-sensitive tumors, thus suggesting that the target for SQMG is *TSP-1* gene expression.

Materials and Methods

Synthesis of SQMG. The chemical structure of the synthesized compound 3′-sulfoquinovosyl-1′-monoacylglycerol (SQMG) containing fatty acid 18:1 (oleic acid: C18:1) is shown in Figure 1(a). The procedure for the synthesis of SQMG was described previously.[14]

Cell lines. Human breast adenocarcinoma MDA-MB-231 was provided by the Japanese Cancer Research Resources Bank. The cells were cultured with DMEM supplemented with 10% FCS, 100 unit/mL penicillin, 100 μg/mL streptomycin, and 2 mM L-glutamine. Human esophagus squamous cell carcinoma TE-8 was obtained from the Health Science Research Resources Bank (Sendai, Japan). These cells were cultured with RPMI 1640 supplemented with 10% FCS, 100 unit/mL penicillin, 100 μg/mL streptomycin and 2 mM L-glutamine.

Establishment of stable transfectants. Total RNA derived from human umbilical vein endothelial cells (HUVEC) (Cambrex, Walkerville, MD, USA) was converted to cDNA by a Transcriptor First Strand cDNA Synthesis Kit (Roche Applied Science, Mannheim, Germany), which was used to obtain human TSP-1 cDNA by PCR amplification with the following primer sets: forward primer, 5′-GCACCAACAGCTCCACCATG-3′ and reverse primer, 5′-GGGATCTCTACATTCGTATT-3′. The amplified fragment was cloned using the pCR4-TOPO cloning vector

[4]To whom correspondence should be addressed.
E-mail: sahara@azabu-u.ac.jp

doi: 10.1111/j.1349-7006.2012.02333.x

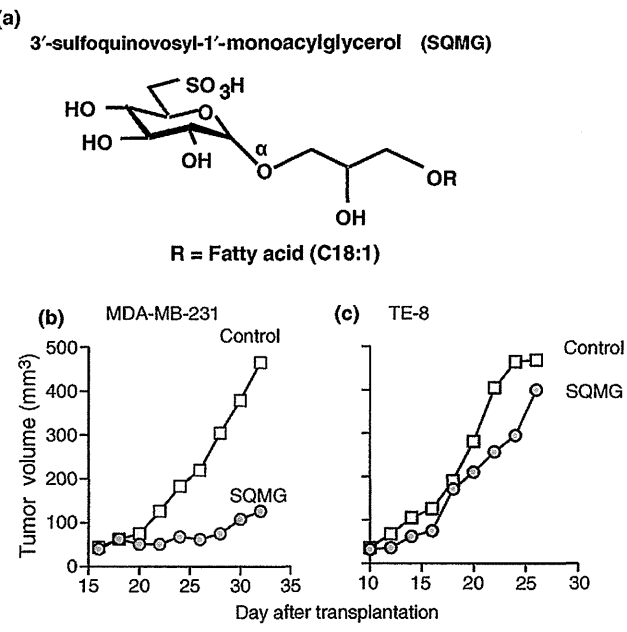

Fig. 1. 3′-sulfoquinovosyl-1′-monoacylglycerol (SQMG) structure and *in vivo* assessment of SQMG for cDNA microarrays study. (a) Structure of SQMG. 3′-sulfoquinovosyl-1′-monoacylglycerol contains a single fatty acid, R = C18:1. 10^6 tumor cells of MDA-MB-231 (b) or TE-8 (c) were subcutaneously injected into mice. When the solid tumors grew to 30–40 mm^3 in tumor volume, mice were injected with SQMG at a dose of 20 mg/kg (SQMG 20) or saline (control) daily for 14 days. Tumor volume from each mouse is shown.

(Invitrogen, Carlsbad, CA, USA), and reconstructed with pcDNA3.1 (Invitrogen) at the *HindIII/XhoI* site. TE-8 cells were transfected with TSP-1 cDNA in the pcDNA3.1 vector, and selected and cloned in a 0.5 mg/mL G418-containing medium (Invitrogen). Several clones were established (TSP1-OT).

We designed five shRNAs and used the Mission*RNAi* (Sigma-Aldrich, St. Louis, MO, USA) technology platform to stably knockdown *TSP-1* gene expression in MDA-MB-231 cells. These sequences were as follows: sh-1, 5′-CCGGATCATCTGGTATACCATTGCCCTCGAGGGCAATGGTATACCAGATGATTTTTTG-3′, sh-2, 5′-CCGGGTAACAGAAACTCGAGTTTCTGTTACATCACCAACGCTTTTTG-3′, sh-3, 5′-CCGGCGATGACATCTGTCCTGAGAACTCGAGTTCTCAGGACAGATGTCATCGTTTTTG-3′, sh-4, 5′-CCGGCCTTGACAACAACGTGGTGAACTCGAGTTCACCACGTTGTTGTCAAGGTTTTTG-3′, sh-5, 5′-CCGGCTCTCAAGAAATGGTGTTCTTCTCGAGAAGAACACCATTTCTTGAGAGTTTTTG-3′. The five shRNAs were cloned into the pLKO.1-puro shRNA vector. Plasmid DNA, including non-targeting shRNA as a control (sh-control), was transfected into the MDA-MB-231 cells along with Lentiviral Packaging Mix (Sigma-Aldrich), which consists of an envelope and packaging vector to produce lentivirus packed with shRNA cassettes, using the standard procedure. After transfection, cells were cultured and cloned in the presence of 5 μg/mL puromycin.

***In vivo* assessment of anti-tumor assay.** Inbred female BALB/c nu/nu mice (20–22 g, 7 weeks old) were obtained from Japan SLC, Inc. (Shizuoka, Japan). All procedures were performed in compliance with the guidelines of the Animal Research Committee of Azabu University. Cells (10^6 cells/mouse) suspended in phosphate-buffered saline (PBS) were injected subcutaneously into the dorsal region of the mice. After implantation, the tumor sizes were measured at 2-day intervals in each mouse. When the solid tumors grew to 30–40 mm^3 in tumor volume (tumor volume = length × [width]^2 × 0.5), SQMG was administrated daily for 14 days, and tumor growth was observed. Each type of tumor was divided randomly into two groups (n = 1, 3, or 4 per group). Mice in the control group were intraperitoneally injected with 0.2 mL of saline solution, and mice in the test groups were intraperitoneally injected with SQMG at a dose of 20 mg/kg daily for 14 days. On the day after the last administration of SQMG, the tumor size was measured, and the tumors were excised and prepared for further study. The mean ± SE of the tumor volume of each group (n = 4 per group) was calculated. The growth of each tumor was analyzed using Student's t-test.

Immunohistochemical study. All of the tumors excised from the mice (n = 4 per group) were embedded in Tissue-Tek O.C.T. Compound (Sakura Finetek USA, Torrance, CA, USA) and frozen. Acetone-fixed cryosections were stained with an anti-mouse CD31 mAb, followed by anti-rat IgG conjugated with AlexaFlour 488 (BD Bioscience Pharmingen, San Jose, CA, USA) as a secondary antibody. Nuclei were counterstained with propidium iodide (PI) (Vector Laboratories, Burlingame, CA, USA). The CD31-positive/ring-form blood vessels in 500-mm^2 section areas of these samples were counted at 100× magnification under a fluorescence microscope (Olympus AX80, Olympus, Tokyo, Japan). The data are represented as a mean ± SE of four section areas from each group, and the results were analyzed using Student's t-test.

MTT assay. To investigate the cell growth of the transfectants, the MTT assay was performed according to the methods described previously.[14] Briefly, cells (5 × 10^3 cells per well) were cultured in 96-well plates for 24 h and different amounts of SQMG suspended in PBS were then added to the wells. After cultivation for 48 h, 50 μg of MTT was added to the cells and incubation was continued for 3 h. Next 4% HCl in 2-propanol was added to each well and mixed using a pipette to disrupt the cells. The absorbance of the contents in each well was measured using a multiwell scanning photometer (Micro ELISA MR600; Dynatech Laboratories, Alexandria, VA, USA) at a wavelength of 570 nm. Results are represented as a mean ± SE of triplicate wells for one of three independent experiments.

Gene expression profiling using cDNA microarrays. We isolated total RNA from the xenografted solid tumors in mice in accordance with protocols recommended by Affymetrix (Santa Clara, CA, USA) for GeneChip experiments. Total RNA was isolated using the RNeasy Mini Kit (Qiagen, Hilden, Germany) according to the manufacturer's instructions, reverse-transcribed to cDNA with a Transcriptor First Strand cDNA Synthesis Kit (Roche Applied Science), and then labeled with a biotinylated nucleotide analog (pseudouridine base). The labeled cDNA products were fragmented, loaded on to the Human Genome U133 Plus 2.0 Array (Affymetrix) and hybridized according to the manufacturer's protocol. The GeneChip array data were analyzed using the DNA Microarray Viewer, provided by Kurabo Industries (Osaka, Japan), which is the authorized service provider of Affymetrix in Japan.

Quantitative real-time RT-PCR analysis. The quantitative measurement of gene expression was performed using the LightCycler system (Roche Applied Science). Quantitative real-time RT-PCR analyses of human glucose-6-phosphate dehydrogenase (*G6PDH*) and *TSP-1* gene expression were performed using the LightCycler FastStart DNA MasterPLUS SYBR Green I system (Roche Applied Science) with the following primer sets: forward primer, 5′-CTGCGTTATCCTCACCTTC-3′ and reverse primer, 5′-CGGACGTCATCTGAGTTG-3′ for the detection of human *G6PDH*; forward primer, 5′-GATGGAGAATGCTGAGTTG-3′ and reverse primer, 5′-TGAGGAGGACACTGGTAGAG-3′ for the detection of human *TSP-1*. PCR amplification of the housekeeping gene, *G6PDH*, was performed for each sample as a

control for sample loading and to allow for normalization among the samples. To determine the absolute copy number of the target transcripts, the fragments of *G6PDH* or the target genes amplified by PCR using the above described primer sets were subcloned into the pCR4-TOPO- cloning vector (Invitrogen). The concentrations of these purified plasmids were measured by absorbance at 260 nm, and copy numbers were calculated from the concentration of the samples. A standard curve was created by plotting the threshold cycle (C_t) versus the known copy number for each plasmid template in the dilutions. The copy numbers for all unknown samples were determined according to the standard curve using LightCycler version 3.5.3 (Roche Applied Science). To correct for differences in both RNA quality and quantity between samples, each target gene was first normalized by dividing the copy number of the target by the copy number of *G6PDH*; therefore, the mRNA copy number of the target was the copy number per the copy number of *G6PDH*. The initial value was also corrected for the amount of *G6PDH* indicated as 100% to evaluate the sequential alteration of the mRNA expression level.

Assessment of TSP-1 expression *in vitro*. Cells were seeded into six-well plates at a density of 2×10^5 cells/well and cultured overnight. Then cells were cultured in the presence of 25 μM SQMG for 0, 1, 3, 6, 12, or 24 h and then harvested. Total RNAs from these cells were prepared and *TSP-1* gene expression were performed using same methods for xenografted solid tumors *in vivo*.

TSP-1 promoter-reporter constructs and luciferase assay. Human genomes were prepared from MDA-MB-231 cells using the DNeasy Blood and Tissue kit (Qiagen) according to the manufacturer's instructions. A luciferase reporter plasmid containing the −2220 to +750 region of the human *TSP-1* gene promoter was cloned from human genome by PCR system using forward primer, 5′-CAACTGAAGTATCATGATAAGAG-3′ and reverse primer 5′-ATCCTGTAGCAGGAAGCACAAG-3′. To ligate into pGL4.10 vector (Promega, Madison, WI, USA), second PCR as template for first PCR product was performed using forward primer; 5′-GTACCGGTACCCAACTGAAGTATCATGATAAGAG-3′, which was added to 5′-GTACCGGTACC-3′ containing *Kpn*I site and reverse primer; 5′-ATATCCTCGAGATCCTGTAGCAGGAAGCACAAG-3′, which was added to 5′-ATATCCTCGAG-3′ containing *Xho*I site. The PCRs were performed using GoTaq system (Promega). The second PCR product was digested with *Kpn*I and *Xho*I and subcloned into a luciferase plasmid pGL 4.10 vector (TSP1-promoter pGL4.1 plasmid), and their sequences were confirmed by sequencing.

Thrombospondin 1-knocked down MDA-MB-231 cells (TSP1-KD) or sh-control cells were seeded into 24-well plates at a density of 5×10^4 cells/well and cultured overnight. Then cells were transiently cotransfected using Lipofectamine LTX (Invitrogen) with 40 ng pGL4.74 plasmid (hRluc/TK; Promega) as an internal control, and 1 μg target plasmids, such as SV40 promoter pGL 4.13 plasmid (luc2/SV40; Promega) as a positive control, the promoterless pGL 4.10 plasmid as negative vector, or TSP1-promoter pGL 4.10 plasmid. After 24 h of transfection, these cells were cultured with 25 μM SQMG or not for 1, 3, 6, 12 or 24 h. Luciferase activities were assayed using the dual-luciferase assay kit (Promega) according to the manufacturer's directions. The relative luciferase activity for each cell was calculated relative to the activity of the promoterless pGL 4.10 plasmid (negative control). The results were analyzed using Student's *t*-test.

Results

Gene expression profiling using cDNA microarrays. 3′-sulfoquinovosyl-1′-monoacylglycerol-sensitive MDA-MB-231 cells and SQMG-resistant TE-8 cells were subcutaneously injected into mice. Mice bearing solid tumors that grew to 30–40 mm^3 were then intraperitoneally injected with saline or SQMG daily for 14 days. As shown in Figure 1(b), the SQMG treatment in mouse with MDA-MB-231 solid tumor resulted in inhibition of tumor growth as compared with control mouse on the day after the last injection. In contrast, mouse with TE-8 solid tumor treated with SQMG showed no inhibition of tumor growth as compared with control mouse on the day after the last injection (Fig. 1c).

Four solid tumors were harvested, total RNA was prepared and gene expression profiles were analyzed using cDNA microarrays. A subset of the microarray results is shown in Table 1. Genes that were upregulated after SQMG treatment in the SQMG-sensitive tumor MDA-MB-231 samples, as compared with controls, and that also showed no change in expression in the TE-8 sample, regardless of SQMG administration, were identified. Given its known anti-angiogenic effects, we chose to investigate TSP-1 as a potential target of SQMG.[7–9] In order to confirm the upregulation of *TSP-1* gene expression in xenografted tumors in nude mice, we again performed *in vivo* assessment and real-time PCR. Total RNAs derived from four SQMG-sensitive MDA-MB-231 tumors treated with SQMG and three SQMG-sensitive tumors treated without SQMG, and from a total of eight SQMG-resistant TE-8 tumors treated either with or without SQMG, were also harvested. As shown in Figure 2(a), in the SQMG-sensitive MDA-MB-231 tumors, an increased tendency of *TSP-1* expression with SQMG treatment was observed ($P = 0.11$). However, in the SQMG-resistant TE-8 tumors, a difference in expression was not observed (Fig. 2b). Therefore, we further investigated whether SQMG treatment could induce upregulation of *TSP-1* gene expression in MDA-MB-231 and TE-8 cells *in vitro*. Consequently, an increase in *TSP-1* gene expression in MDA-MB-231 was observed from 3 to 12 h after SQMG treatment, and this returned to baseline by 24 h, indicating that the duration of upregulation is short (Fig. 2c). On the other hand, upregulation in TE-8 was not observed. These data suggest that the upregulation of *TSP-1* gene expression is induced by SQMG in SQMG-sensitive MDA-MB-231 cells *in vitro* and that detection in xenografted solid tumors is difficult *in vivo* because the duration of upregulation is short.

Table 1. Results of DNA micro array analysis (gene expression SQMG treatment/control)

	SQMG/control	
	MDA-MB-231	TE-8
ATP-binding cassette, sub-family F, member 2	4.3	1
E2F transcription factor 7	4.3	0.9
Inhibitor of DNA binding 2, dominant negative helix-loop-helix	3.7	0.9
Lysyl oxidase	3	0.9
Gap junction protein, alpha 1, 43 kDa	2.8	1
Egl nine homolog 3 (*C. elegans*)	2.8	0.9
Angiogenin	2.6	0.9
v-myc myelocytomatosis viral oncogene homolog (avian)	2.5	1
Thrombospondin-1	1.7	0.9
Serpin peptidase inhibitor, clade B (ovalbumin), member 5	0.1	0.9
Vitamin D (1,25- dihydroxyvitamin D3) receptor	0.2	1

doi: 10.1111/j.1349-7006.2012.02333.x